Наномеханика

Nanomechanics of materials and systems

Лекции 14

МЭМС и НЭМС:
датчики ускорения и поворота,
нанопривоы, оптические и электронные системы

MEMS and NEMS sensors of acceleration and rotation, actuators, optical and electronic systems

Базовая структура датчика ускорения
Base structure of acceleration sensor

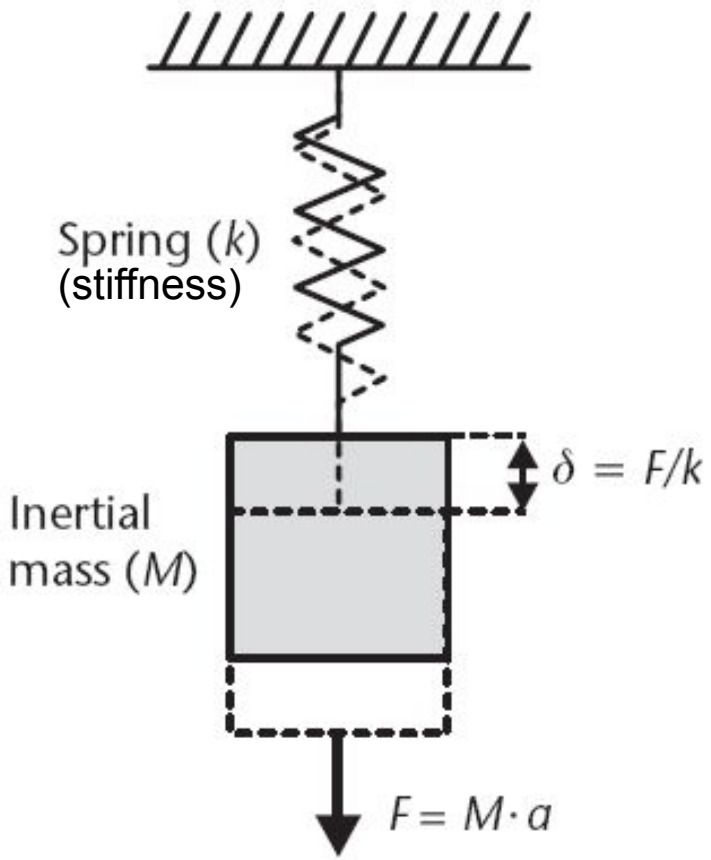

Resonant frequency:

$$f_r = \frac{1}{2\pi}\sqrt{\frac{k}{M}}$$

Noise equivalent acceleration:

$$a_{noise} = \sqrt{\frac{8\pi K_B T f_r B}{Q\,M}} \quad ; \quad B < f_r$$

K_B = Boltzmann constant

T = Temperature

B = Bandwidth

Q = Quality factor

The basic structure of an accelerometer, consisting of an inertial mass suspended from a spring. The resonant frequency and the noise-equivalent acceleration (due to Brownian noise) are given.

Пьезорезистивный датчик ускорения
Piezoresistive acceleration sensor

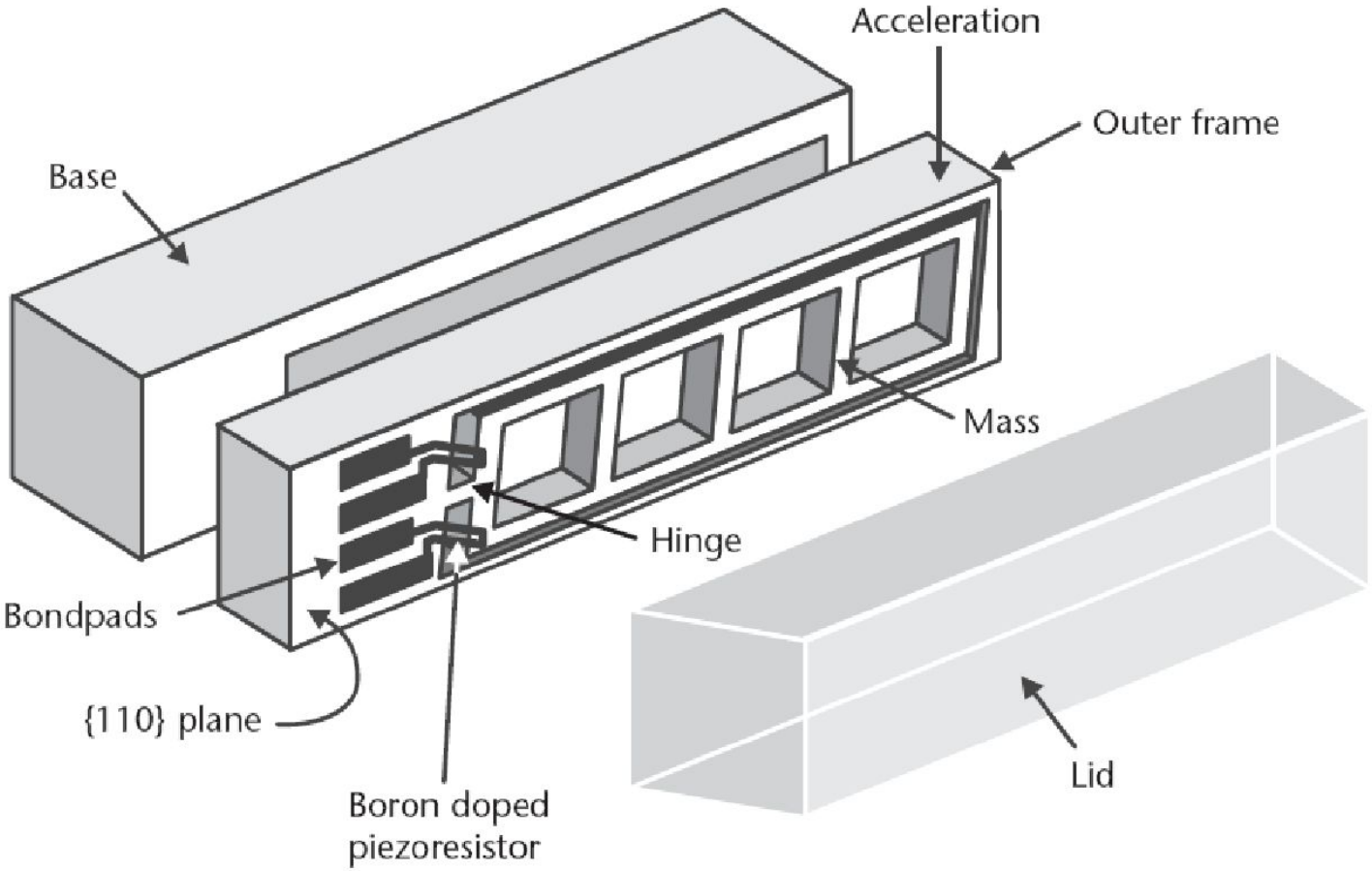

Illustration of a piezoresistive accelerometer from Endevco Corp., fabricated using anisotropic etching in a {110} wafer. The middle core contains the inertial mass suspended from a hinge. Two piezoresistive sense elements measure the deflection of the mass. The axis of sensitivity is in the plane of the middle core. The outer frame acts as a stop mechanism to prevent excessive accelerations from damaging the part. f_r=28 kHz. The piezoresistors are 0.6 μm thick and 4.2 μm long, aligned along <111> direction for maximum performance. The output in response to an acceleration of 1G is 25mV for a Wheatstone bridge excitation of 10V.

Емкостной датчик Capacitive sensor

Поперечная конфигурация

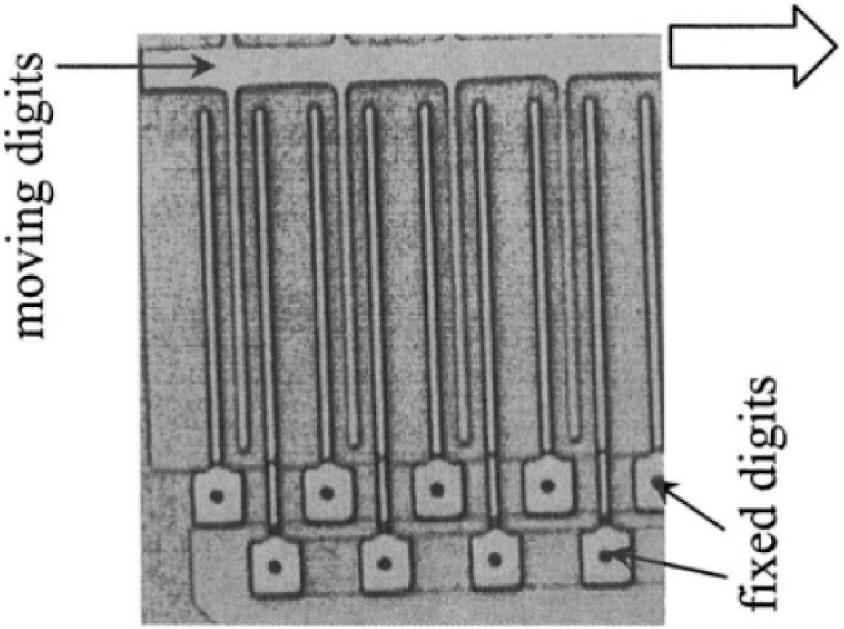

Продольная конфигурация

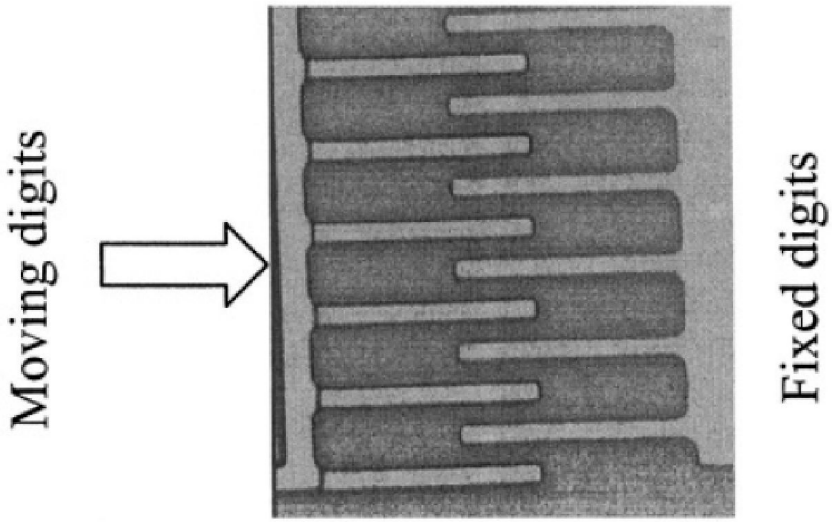

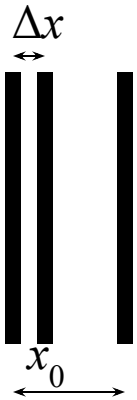

$$U = Q/C; \Delta U = -Q\Delta C/C^2 = -U\Delta C/C$$

$$\Delta C = \frac{\partial C}{\partial x}\Delta x$$

$$\frac{\partial C}{\partial x} = \frac{\varepsilon l_y l_z}{(x_0 - \Delta x)^2}$$

$$\Delta U = -Q\varepsilon l_y l_z / \Delta x$$

$$\Delta U = -U\Delta x/(x_0 - \Delta x)$$

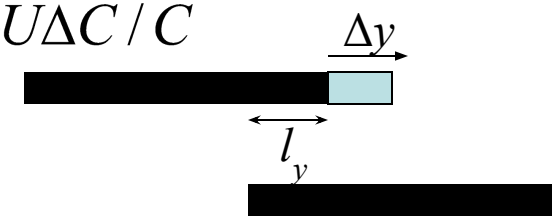

$$C = \varepsilon(l_y + \Delta y)l_z / x_0$$

$$\Delta C = \varepsilon \Delta y l_z / x_0$$

$$\Delta U = -U\Delta y/(l_y + \Delta y)$$

Емкостной датчик ускорения. Capacitive accelerometer.

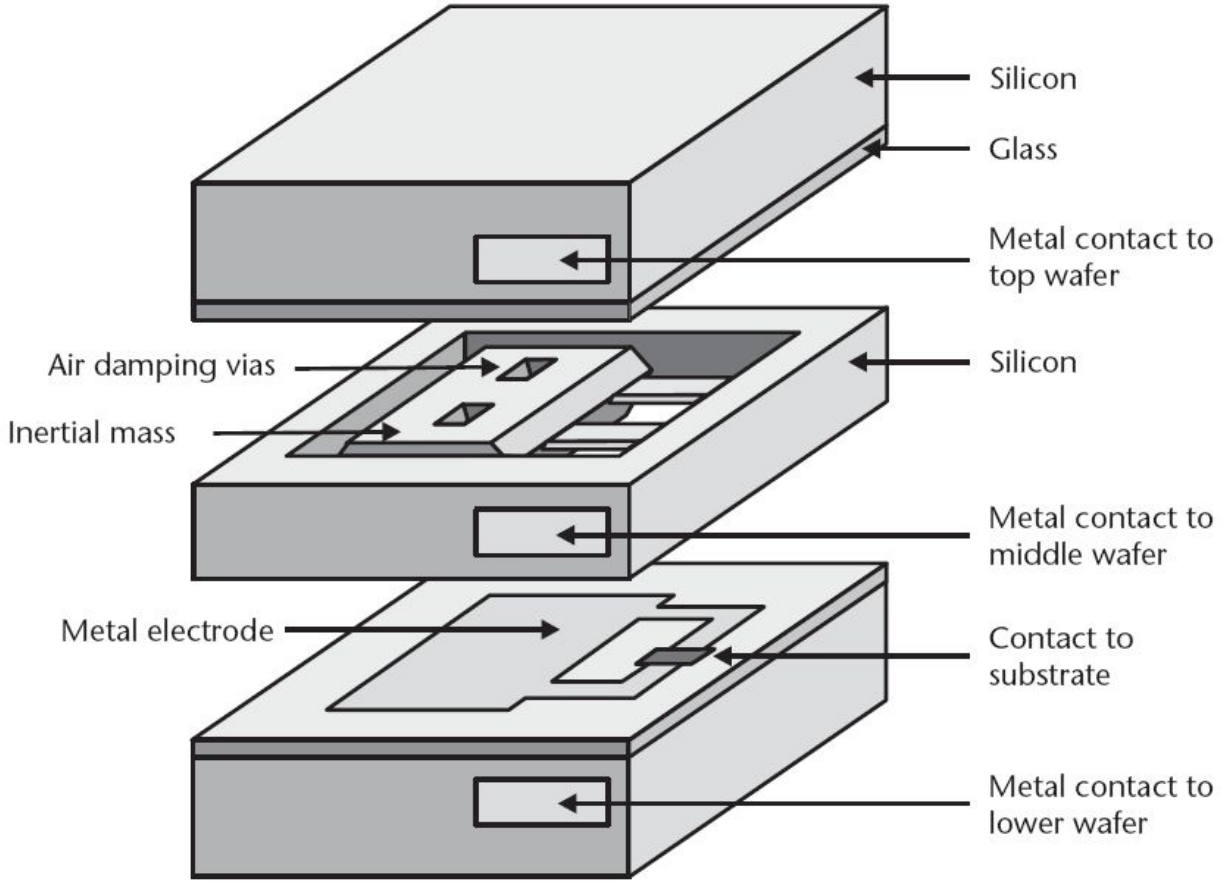

Illustration of a bulk micromachined capacitive accelerometer. The inertial mass in the middle wafer forms the moveable electrode of a variable differential capacitive circuit. Electronic circuits sense changes in capacitance, then convert them into an output voltage between 0 and 5V. The rated bandwidth is up to 400 Hz for the ±12G accelerometer, the cross-axis sensitivity is less than 5% of output, and the shock immunity is 20,000G. Measuring range is from ±0.5G to ±12G. (VTI Technologies of Vantaa, Finland.)

Емкостной датчик ускорения – последовательность производства
Production of capacitive accelerometer

1. Etch recess cavities in silicon

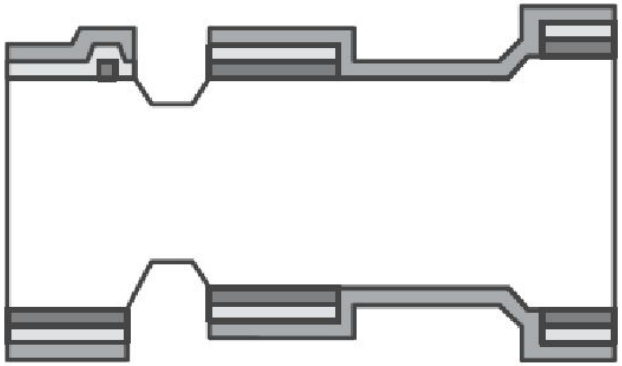

2. Deposit and pattern three masking layers; anisotropic etch silicon

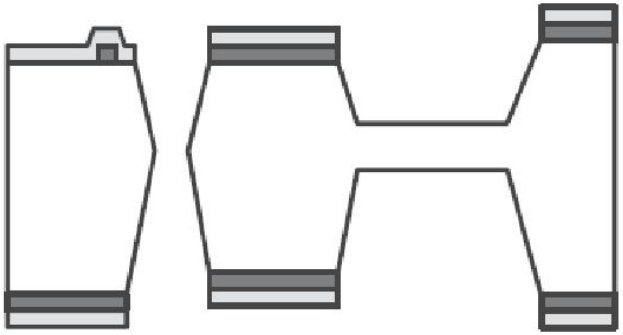

3. Remove first masking layer; anisotropic etch silicon

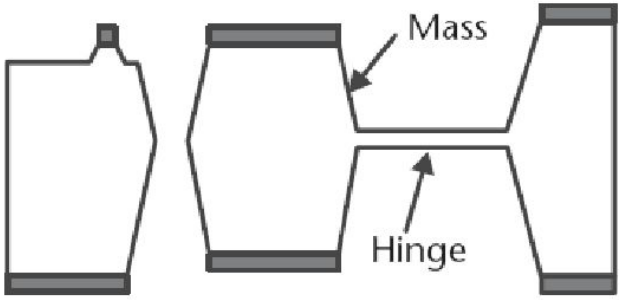

4. Remove second masking layer; anisotropic etch silicon

Емкостной датчик ускорения. Capacitive accelerometer.

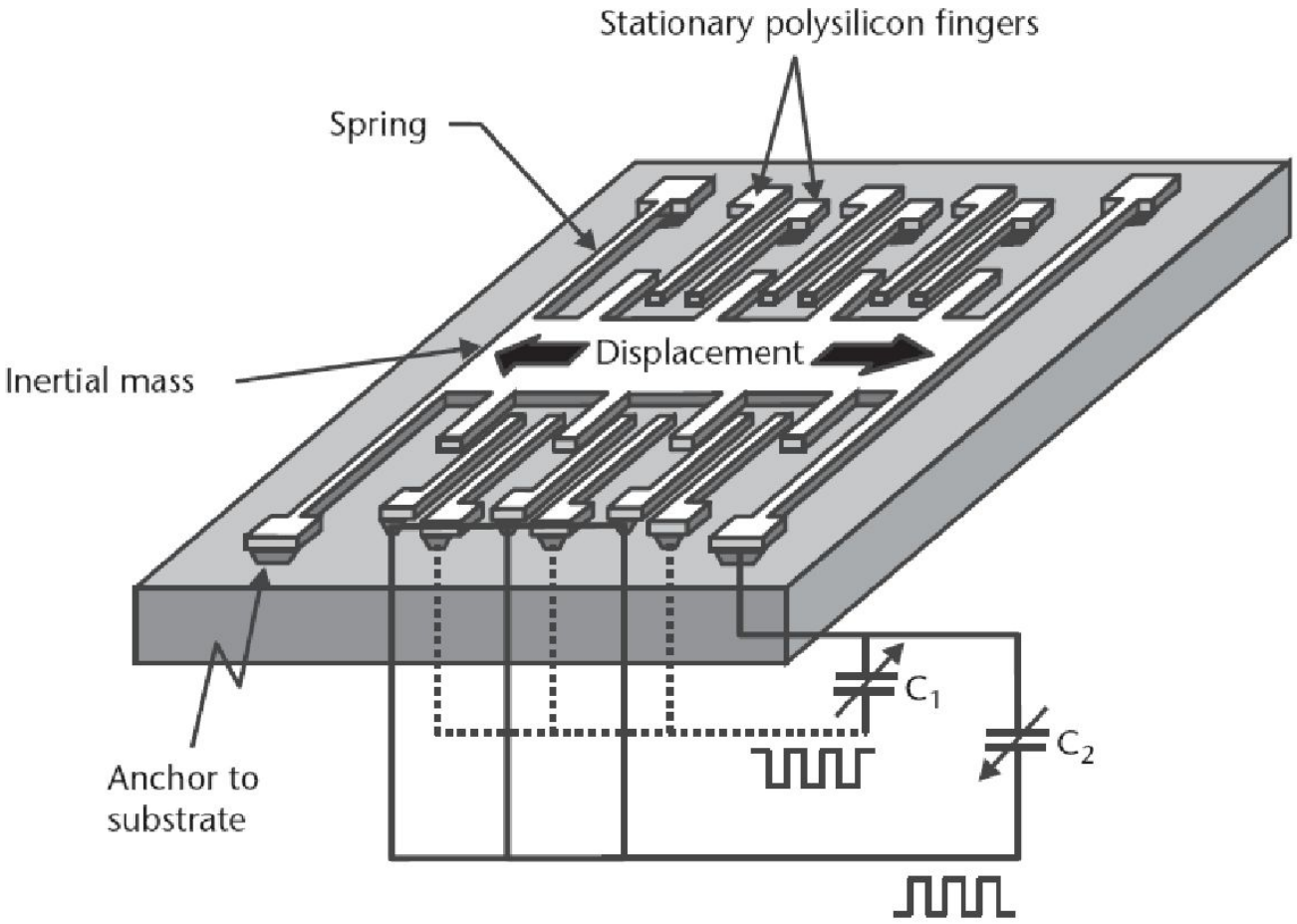

Acceleration rating is from 1G to 100 G, excitation frequency is 1 MHz, C = 10^{-13}F bandwidth is 1-6 kHz, mass is 0.3 - 100 μg, Brownian mechanical noise for 0.3 μg is 225 μ*G Hz*$^{1/2}$

Illustration of the basic structure of the ADXL family of surface micromachined accelerometers. A comb-like structure suspended from springs forms the inertial mass. Displacements of the mass are measured capacitively with respect to two sets of stationary finger-like electrodes. (Analog Devices, Inc., Norwood, Massachusetts, USA.)

Емкостной датчик ускорения, произведенный с помощью DRIE. Capacitive accelerometer using DRIE.

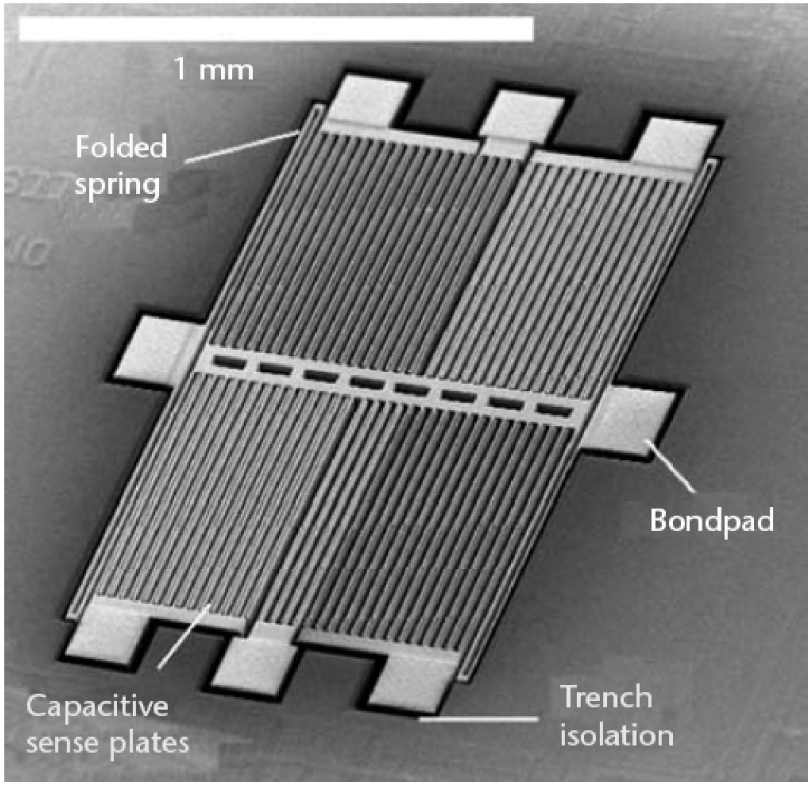

Scanning-electron micrograph of a DRIE accelerometer using 60-μm-thick comb structures. (Courtesy of: GE NovaSensor of Fremont, California.) Using structures 50 to 100 μm deep, the sensor gains an inertial mass, up to 100 μg, and a capacitance, up to 5 pF. The relatively large mass reduces mechanical Brownian noise and increases resolution. The high aspect ratio of the spring practically eliminates the sensitivity to *z*-axis accelerations.

Сравнение пьезорезистивного, емкостного и электромагнитного методов измерения
Comparison of different sensing

Piezoresistive	*Capacitive*	*Electromagnetic*
Simple fabrication	Simple mechanical structure	Structural complexity varies
Low cost	Low cost	Complex packaging
Voltage or current drive	Voltage drive	Current drive
Simple measurement circuits	Requires electronic circuits	Simple control circuits
Low-output impedance	Susceptible to EMI	Susceptible to EMI
High-temperature dependence	Low-temperature dependence	Low temperature dependence
Small sensitivity	Large dynamic range	Sensitivity $\propto$ magnetic field
Insensitive to parasitic resistance	Sensitive to parasitic capacitance	Insensitive to parasitic inductance
Open loop	Open or closed loop	Open or closed loop
Medium power consumption	Low power consumption	Medium power consumption

Элементы НЭМС NEMS elements

- Пассивные Passive
- Датчики Sensors
- Приводы (актуаторы) Actuators

Термический привод Thermal actuator

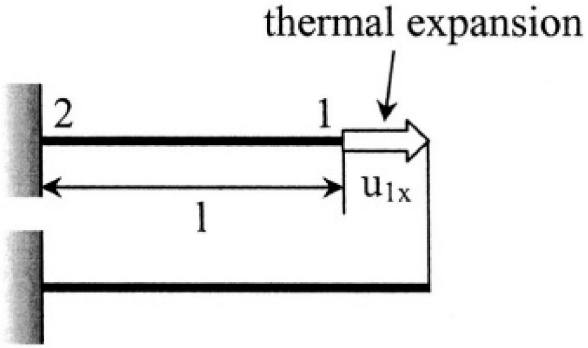

$$F_{1x} = EA\Delta l / l = EA\alpha\Delta T$$

if F is the external force

$$u_{1x} = \alpha l\Delta T - Fl/(EA)$$

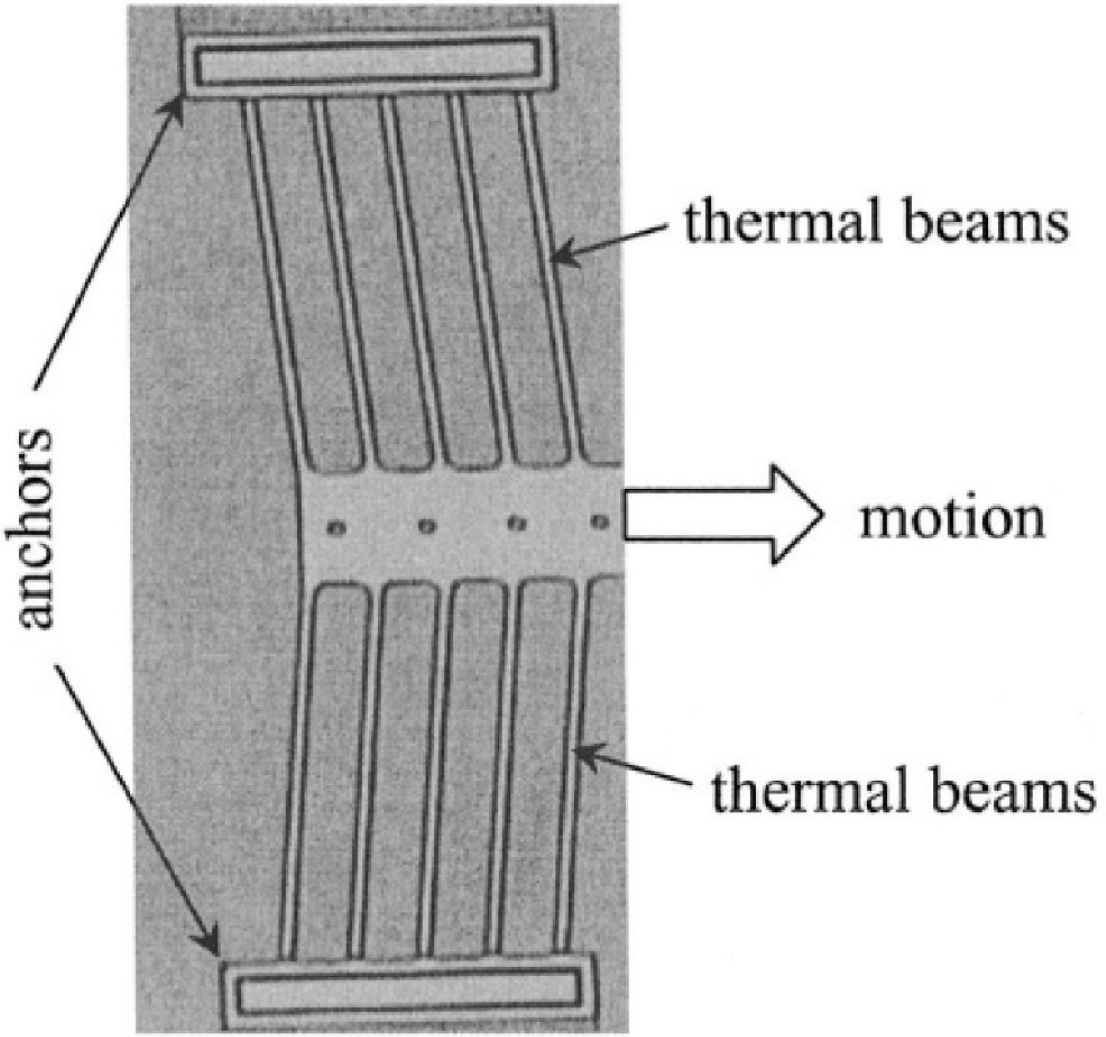

$$u_x = \sqrt{(l+\Delta l)^2 - l^2} \approx \sqrt{2l\Delta l}$$

Пьезоэлектрический элемент (датчик или привод)
Piezoelectric sensor and actuator

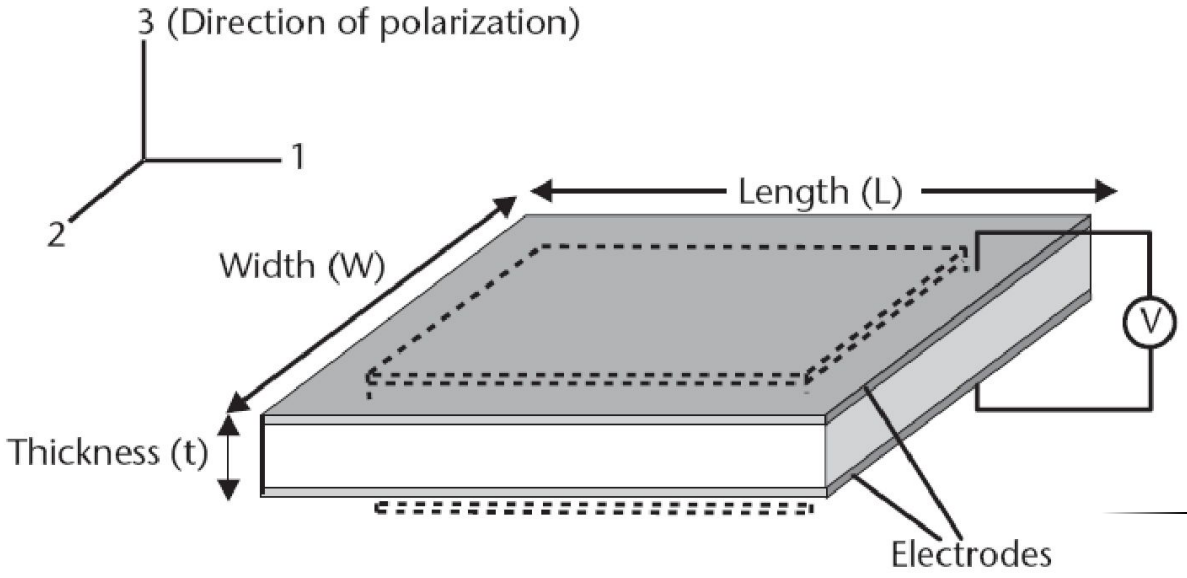

Активный элемент:
ZnO, $LiNbO_3$, $BaTiO_3$, $PbZrO_3$ или кварц

$$\Delta L = d_{31} \cdot V_a \cdot L/t$$

$$\Delta W = d_{31} \cdot V_a \cdot W/t$$

$$\Delta t = d_{33} \cdot V_a$$

An illustration of the piezoelectric effect on a crystalline plate. An applied voltage across the electrodes results in dimensional changes in all three axes (if d_{31} and d_{33} are nonzero). Conversely, an applied force in any of three directions gives rise to a measurable voltage across the electrodes.

$$V_m = d_{31} \cdot F/(\varepsilon \cdot W)$$

$$V_m = d_{31} \cdot F/(\varepsilon \cdot L)$$

$$V_m = d_{33} \cdot F \cdot t/(\varepsilon \cdot L \cdot W)$$

Электростатический нанопривод
Electrostatic actuator

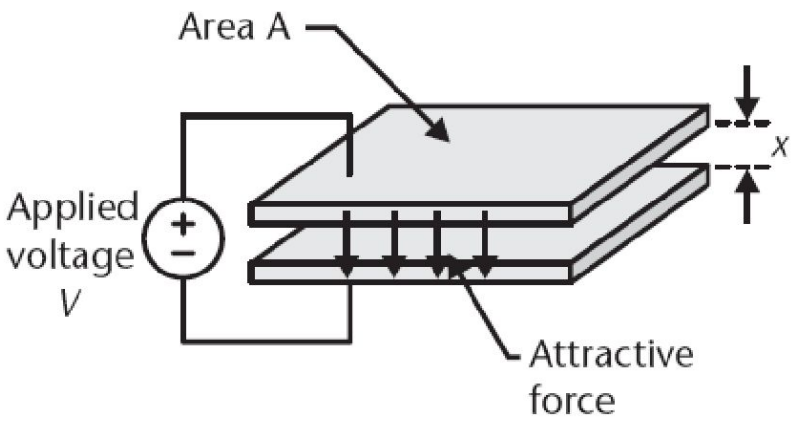

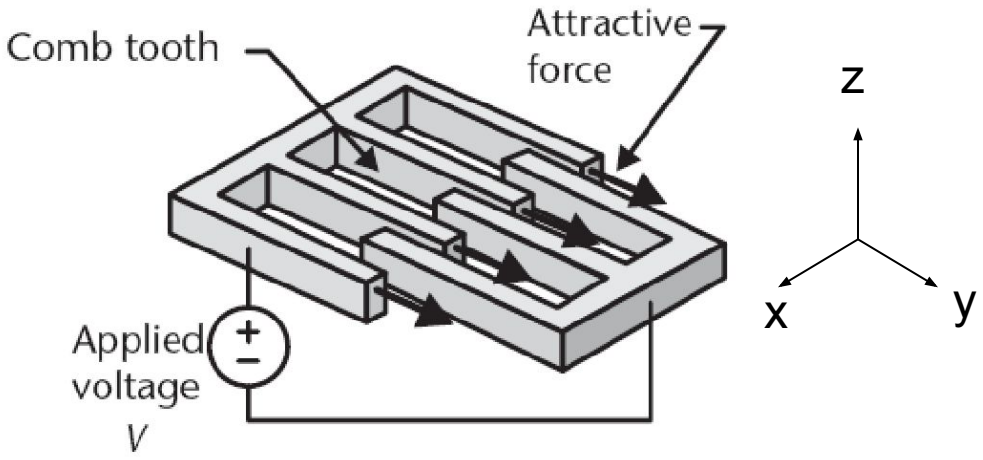

(a)

$$F = \frac{\partial U}{\partial x} = \frac{\varepsilon y_0 z_0 V^2}{(x_0 - \Delta x)^2}$$

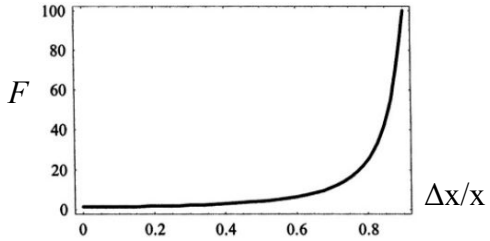

(b)

$$F = \frac{\partial U}{\partial y} = n\frac{\varepsilon z_0 V^2}{2x_0}$$

(a) An illustration of a parallel-plate electrostatic actuator with an applied voltage *V* and a spacing *x*. The attractive force is normal to the plate surfaces. (b) An illustration of an electrostatic comb actuator. The attractive force is in the direction of the interdigitated teeth.

Сравнение различных нанопривводов
Comparison of different nanoactuators

Actuation	*Max. Energy Density*	*Physical and Material Parameters*	*Estimated Conditions*	*Approximate Order (J/cm^3)*
Electrostatic	$\frac{1}{2}\,\varepsilon_0 E^2$	E = electric field ε_0 = dielectric permittivity	5 V/μm	~ 0.1
Thermal	$\frac{1}{2}\,Y(\alpha\,\Delta T)^2$	α = coefficient of expansion ΔT = temperature rise Y = Young's modulus	3×10^{-6} /°C 100°C 100 GPa	~ 5
Magnetic	$\frac{1}{2}\,B^2/\mu_0$	B = magnetic field μ_0 = magnetic permeability	0.1 T	~ 4
Piezoelectric	$\frac{1}{2}\,Y(d_{33}\,E)^2$	E = electric field Y = Young's modulus d_{33} = piezoelectric constant	30 V/μm 100 GPa 2×10^{-12} C/N	~ 0.2
Shape-memory alloy	—	Critical temperature		~ 10 (from reports in literature)

Гироскопы и датчики поворота
Gyroscopes and tilt sensors

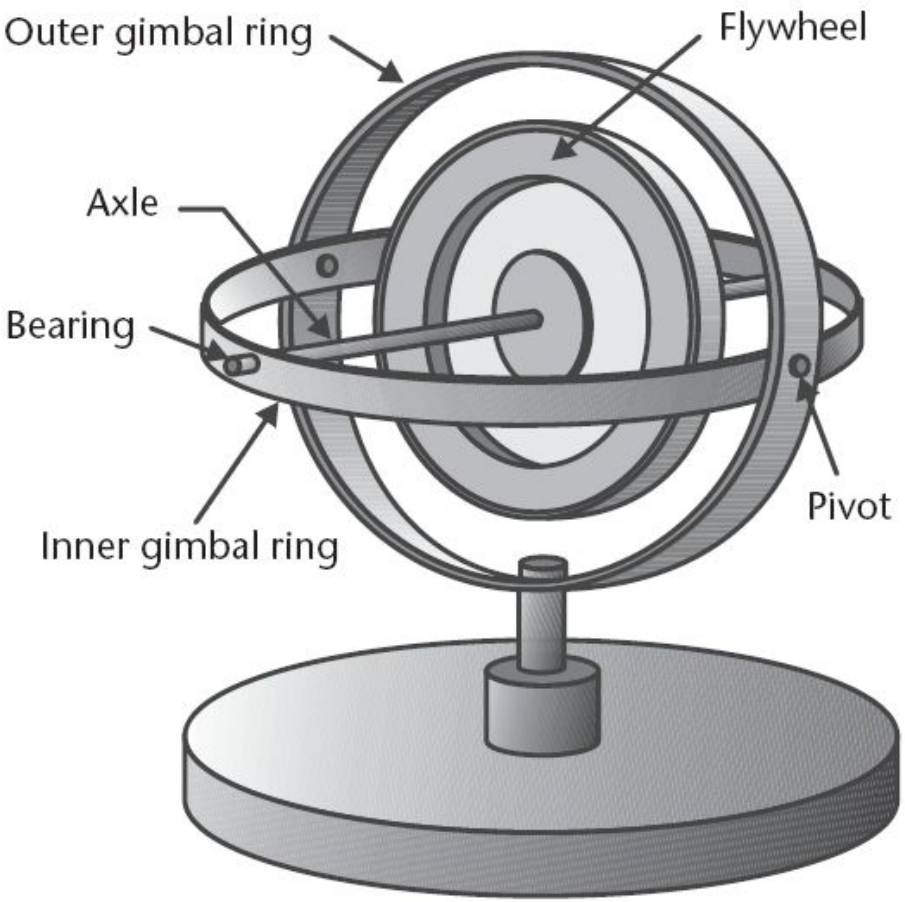

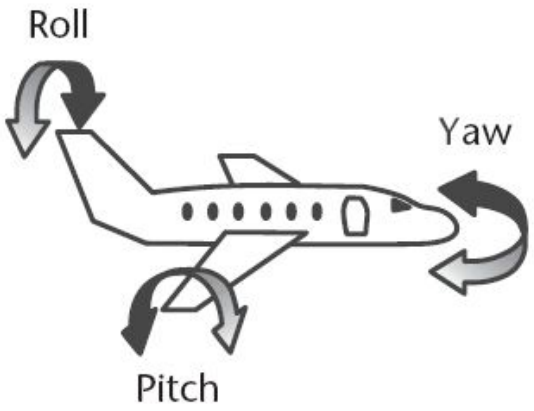

Кориолисово ускорение Coriolis acceleration

v_{Earth}= 1670 cos(lattitude) km/h

Seattle, Washington (lat. 48º N),
v_{Earth}= 1120 km/h
to Los Angeles, California (lat. 34º N)
v_{Earth}= 1385 km/h

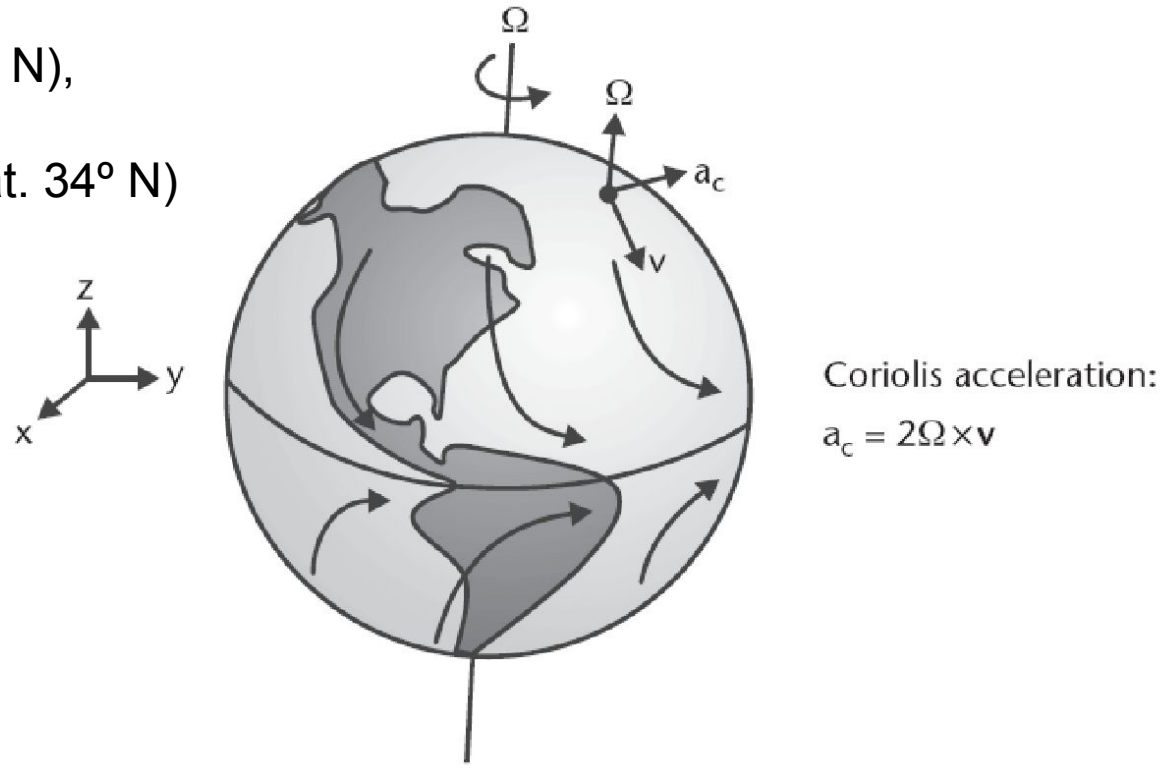

Illustration of the Coriolis acceleration on an object moving with a velocity vector **v** on the surface of Earth from either pole towards the equator. The Coriolis acceleration deflects the object in a counterclockwise manner in the northern hemisphere and a clockwise direction in the southern hemisphere. The vector Ω represents the rotation of the planet.

Базовый датчик угловой скорости
Base angular rate sensor

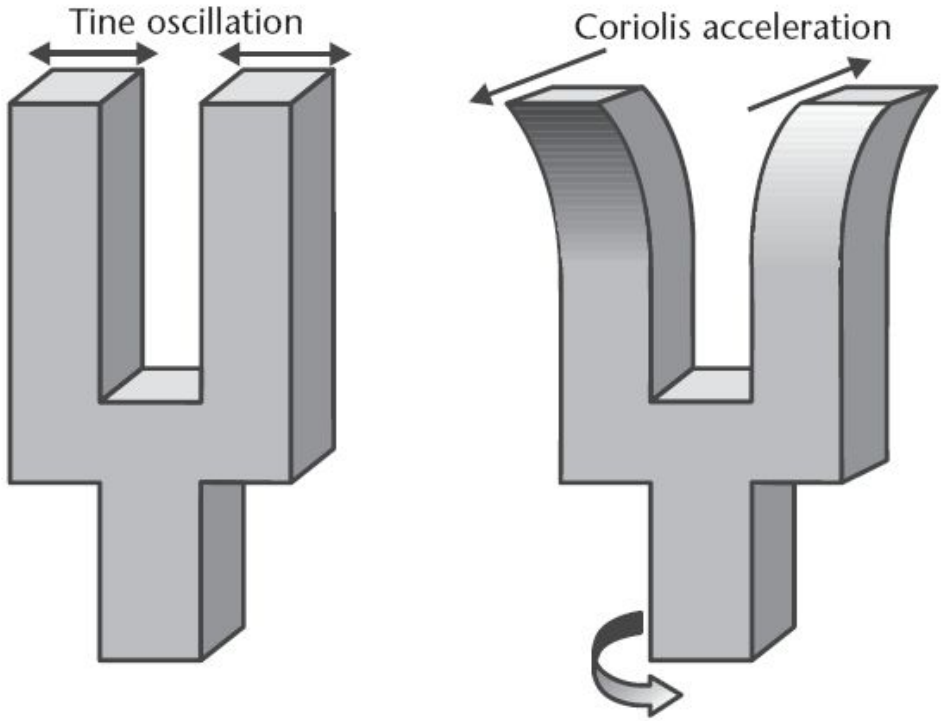

Illustration of the tuning-fork structure for angular-rate sensing. The Coriolis effect transfers energy from a primary flexural mode to a secondary torsional mode. Coriolis acceleration $a_c = 2\Omega \times \mathbf{v}$.

Датчик угловой скорости Angular-rate sensor

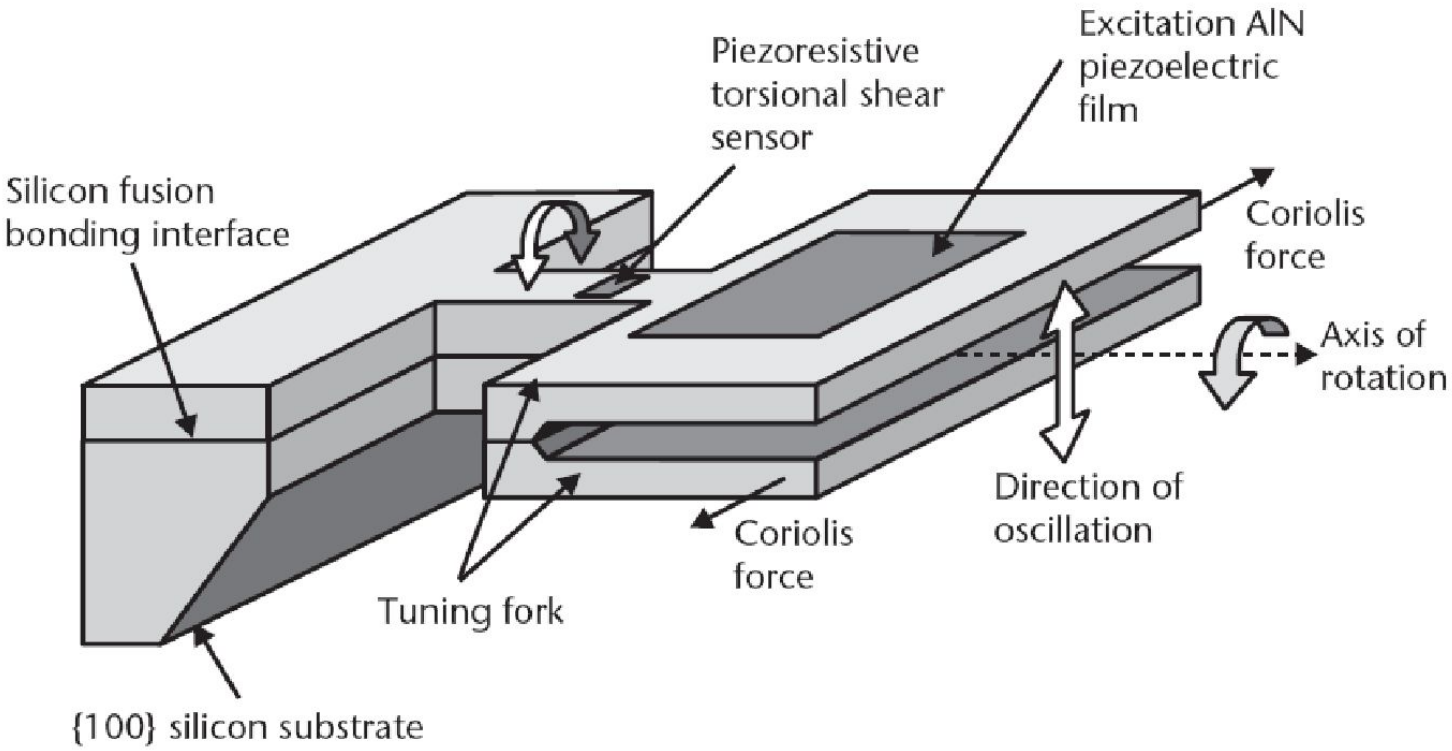

Illustration of the angular-rate sensor from Daimler Benz. The structure is a strict implementation of a tuning fork in silicon. A piezoelectric actuator excites the fork into resonance. The Coriolis force results in torsional shear stress in the stem, which is measured by a piezoresistive sense element. The measured frequency of the primary, flexural mode (excitation mode) is 32.2 kHz, whereas the torsional secondary mode (sense mode) is 245 Hz lower.

Датчик угловой скорости Daimler Benz – последовательность производства
Angular-rate sensor – fabrication steps

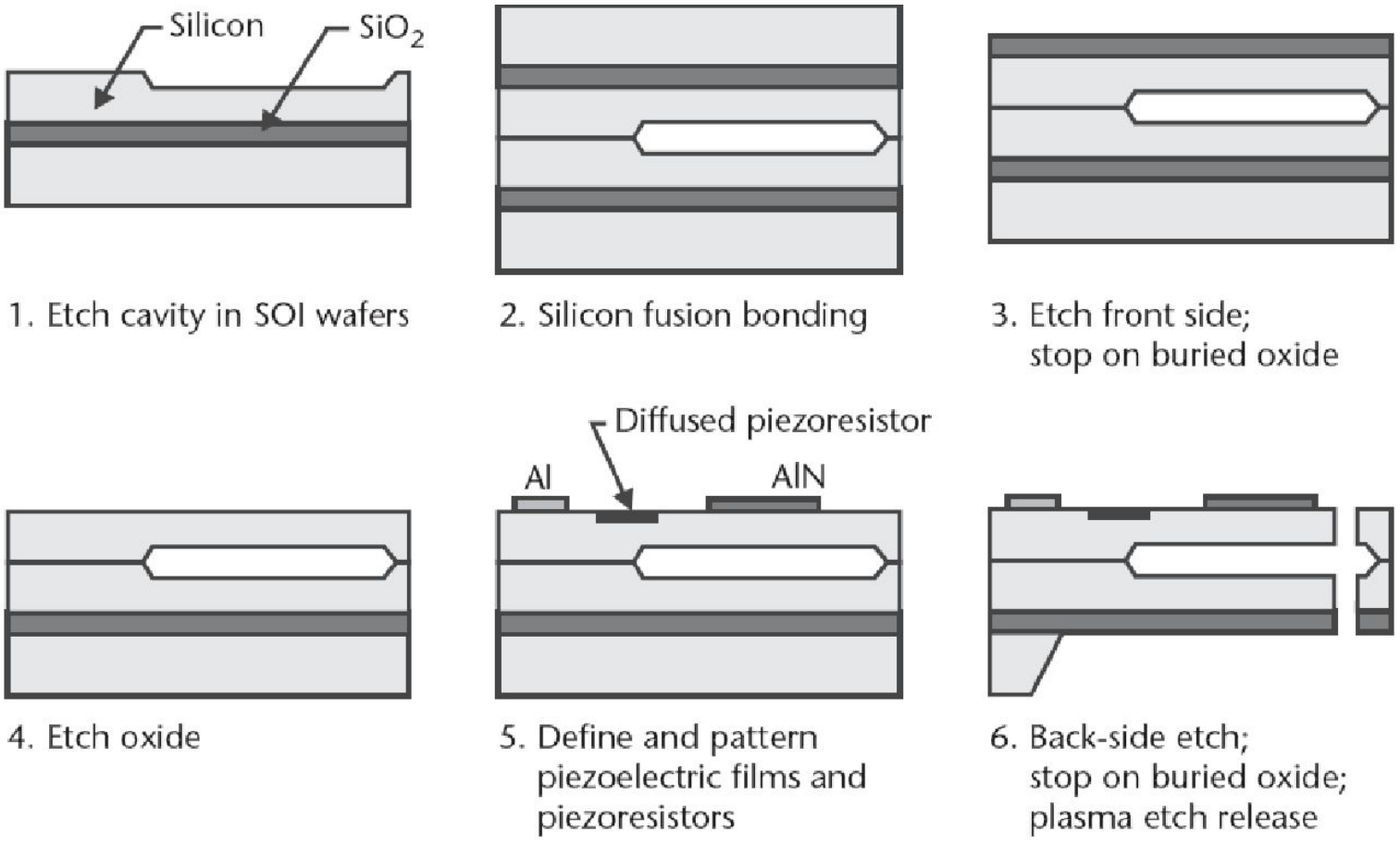

1. Etch cavity in SOI wafers
2. Silicon fusion bonding
3. Etch front side; stop on buried oxide
4. Etch oxide
5. Define and pattern piezoelectric films and piezoresistors
6. Back-side etch; stop on buried oxide; plasma etch release

Датчик угловой скорости Angular-rate sensor

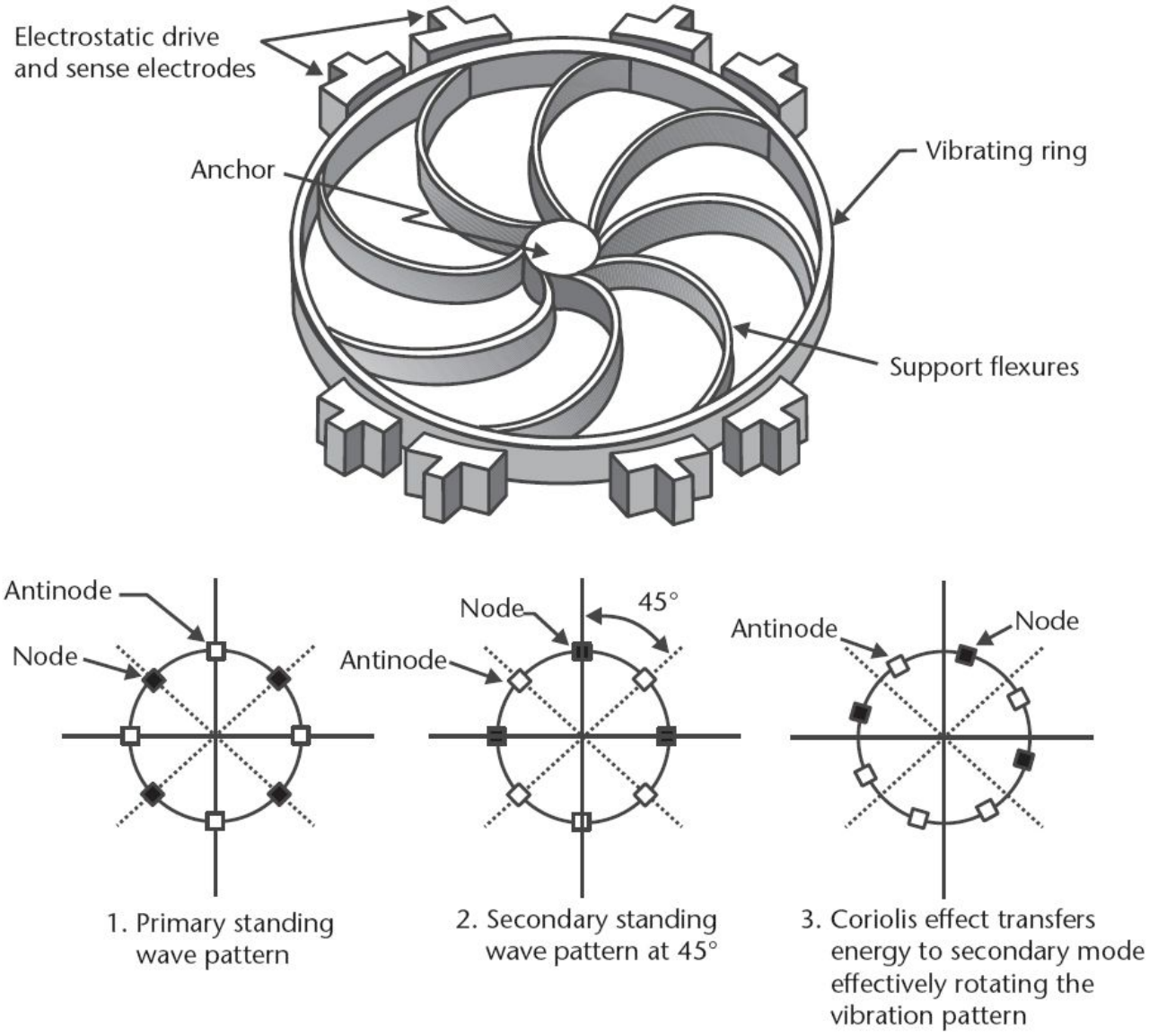

Illustration of the Delphi Delco angular-rate sensor and the corresponding standing-wave pattern. The basic structure consists of a ring shell suspended from an anchor by support flexures. A total of 32 electrodes (only a few are shown) distributed around the entire perimeter of the ring excite a primary mode of resonance using electrostatic actuation. A second set of distributed electrodes capacitively sense the vibration modes. The angular shift of the standing-wave pattern is a measure of the angular velocity.

Датчик угловой скорости Angular-rate sensor

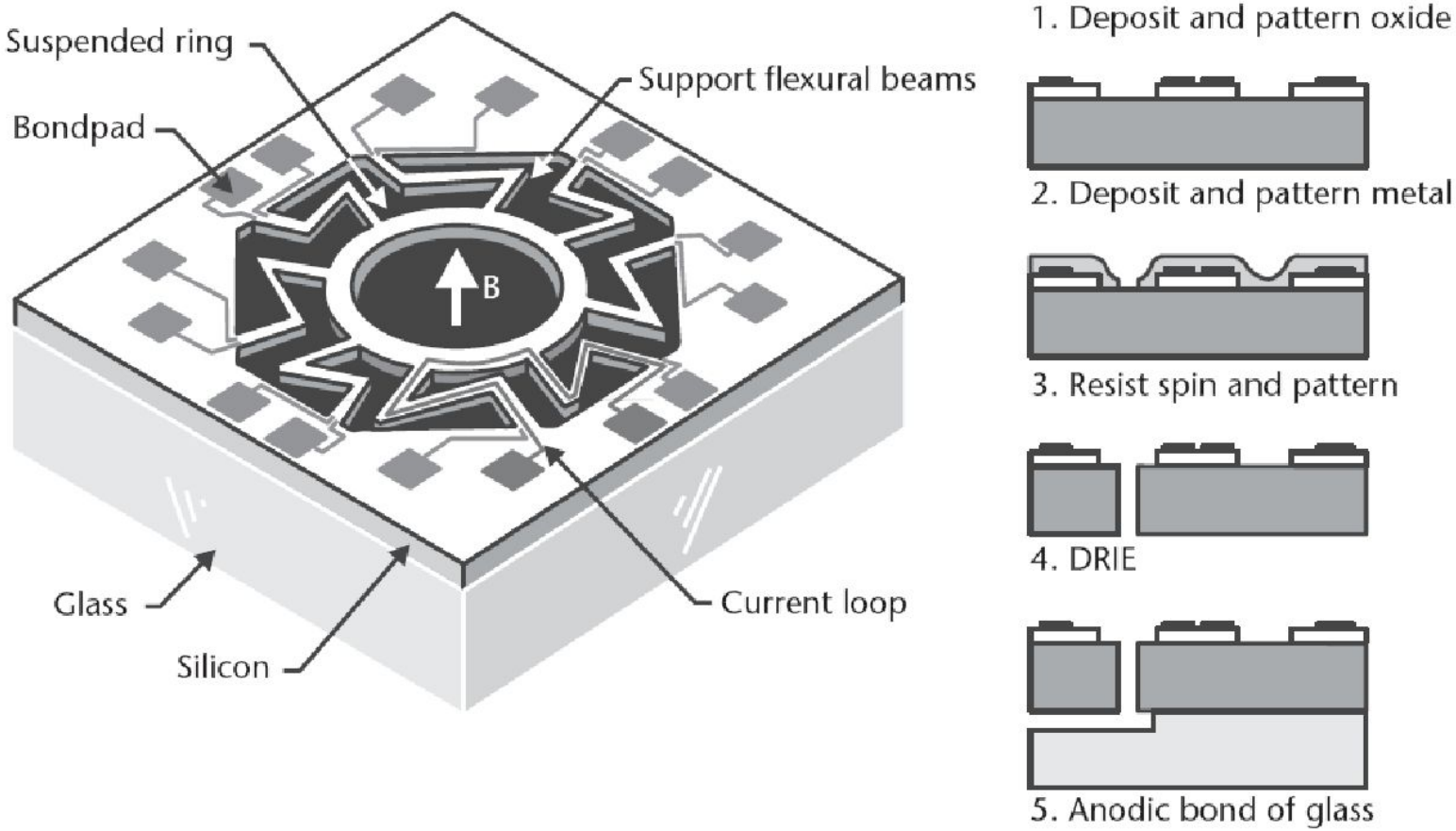

Illustration of the CRS angular-rate sensor from Silicon Sensing Systems (UK&Jp) and corresponding fabrication process. The device uses a vibratory ring shell design, similar to the Delphi Delco sensor. Eight current loops in a magnetic field, *B*, provide the excitation and sense functions. For simplicity, only one of the current loops is shown.

Микро/наногенераторы: Vibration Harvesting

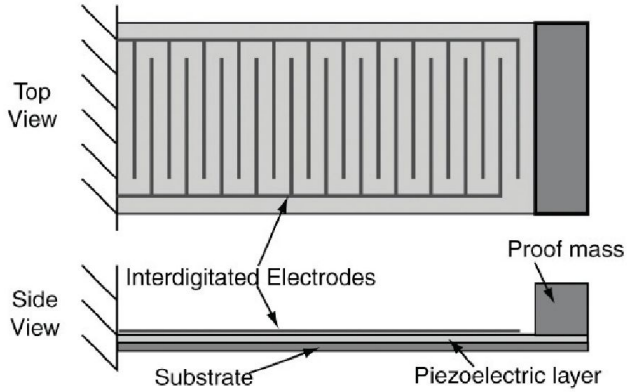

Illustration: Not to scale

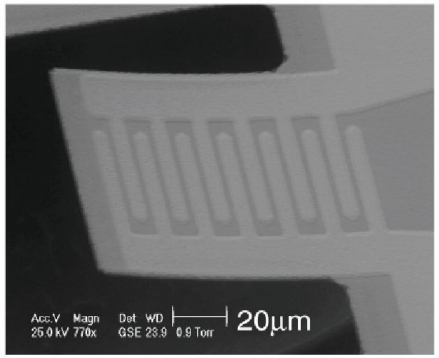

SEM of prototype device

Illustration of unimorph configuration (left) and SEM of a prototype device (right, courtesy of S.-G. Kim).

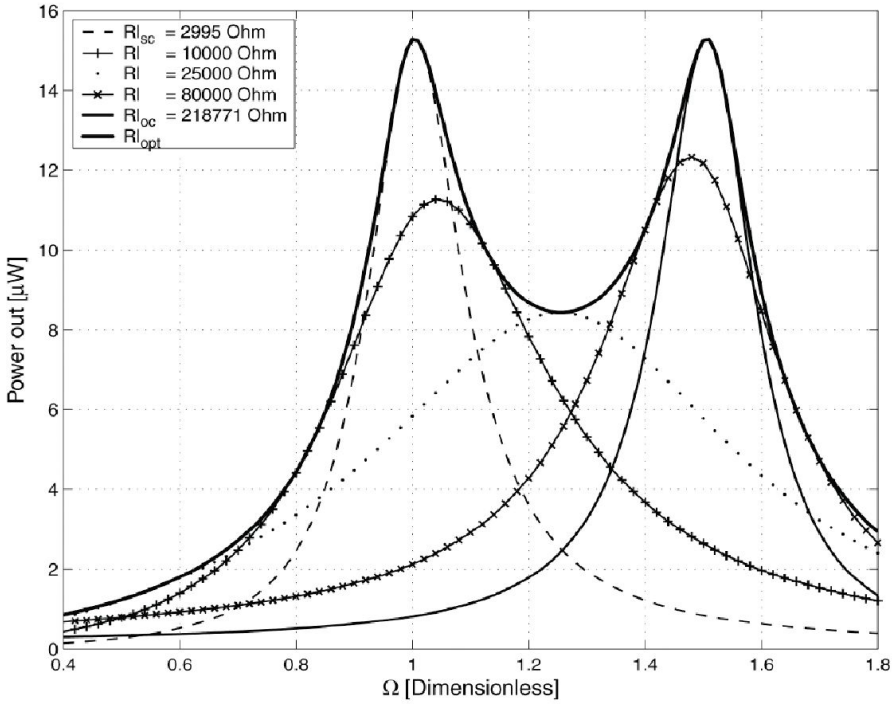

Vibrations generate 10’s-100’s of µW

Power vs. normalized frequency with varying electrical load resistance

Self-powered Wireless Corrosion-monitoring System

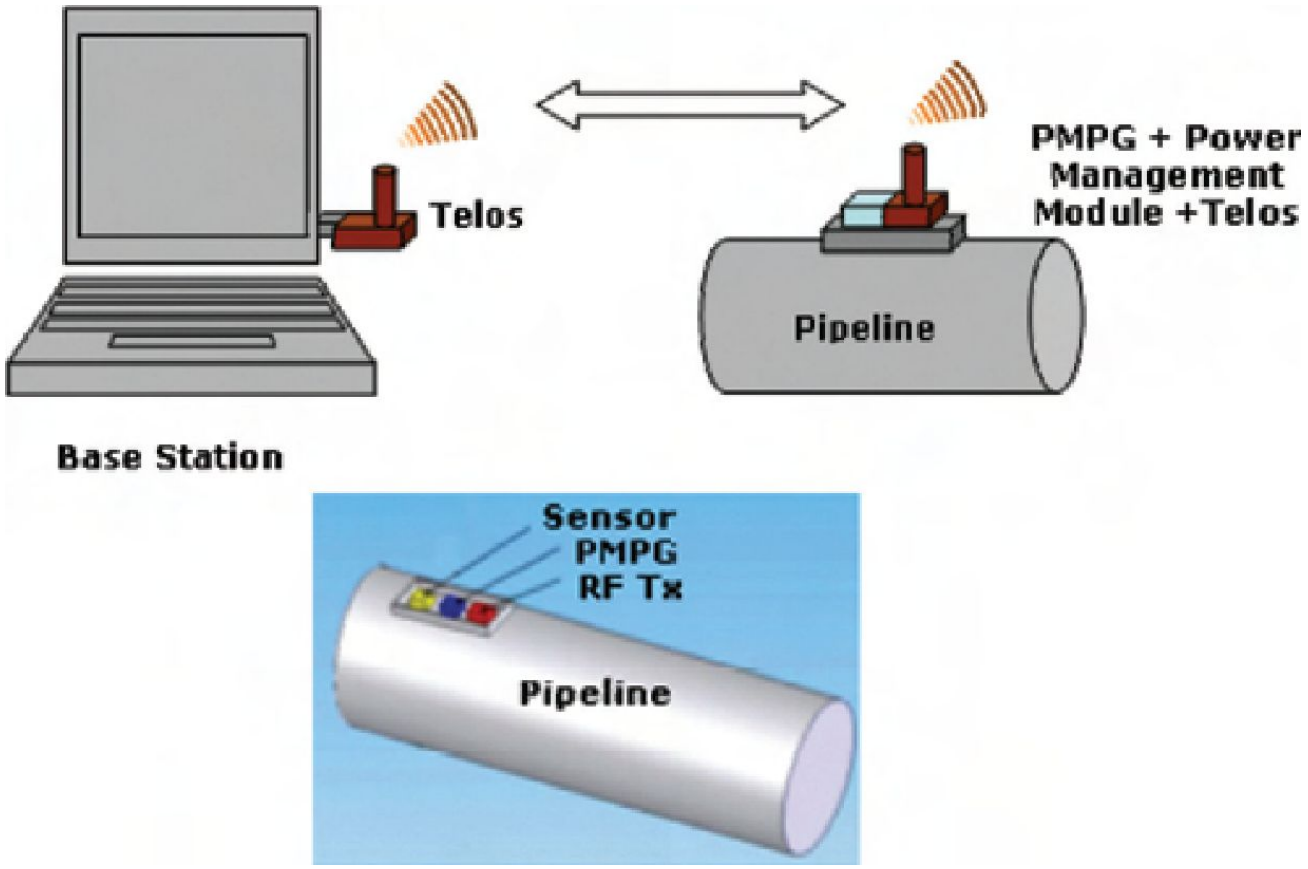

Wireless sensor system schematics. The selfpowered sensor node transmits data to a receiver at the base station.

Оптические переключатели Optical switches

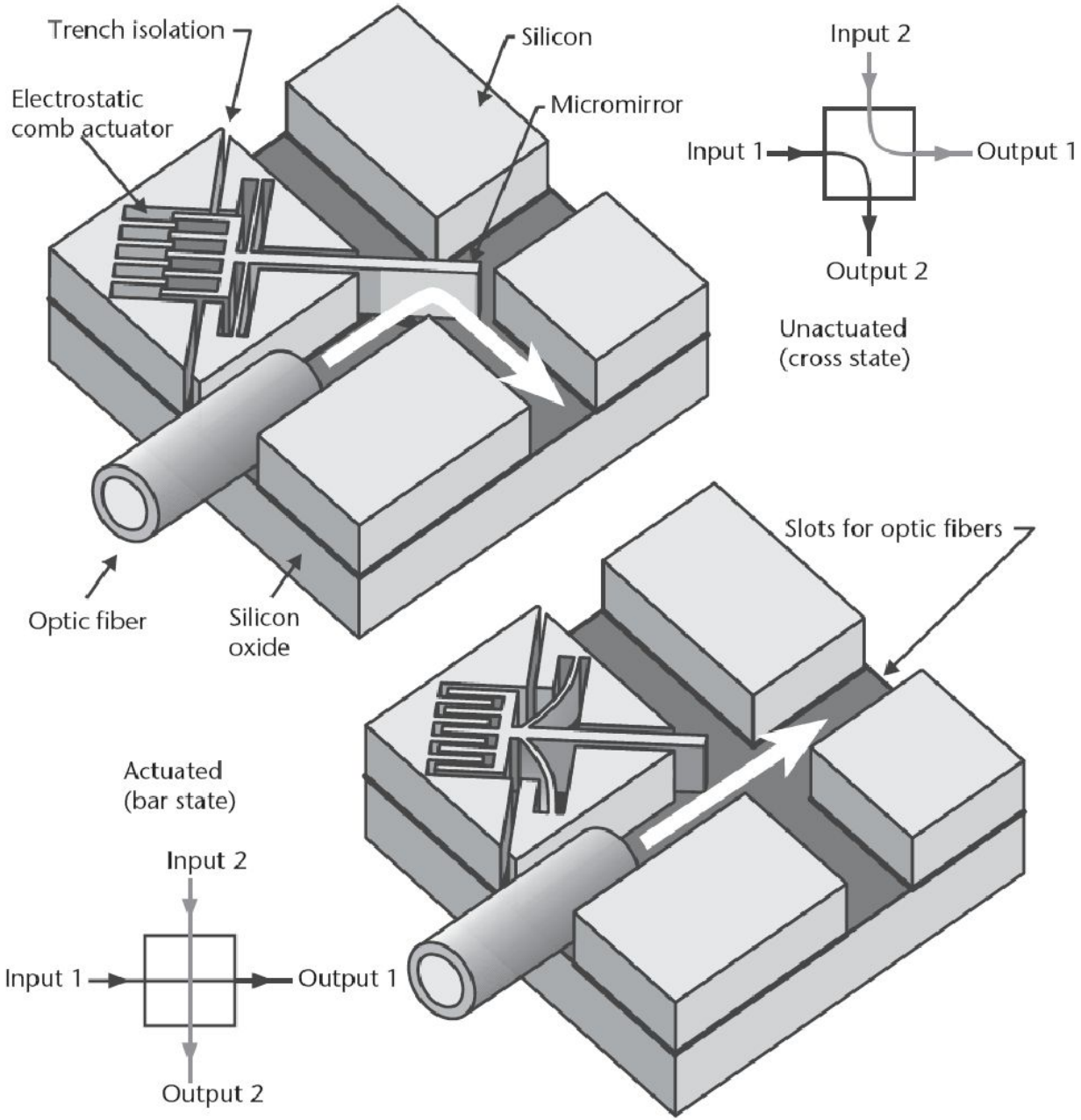

Illustration of a 2 x 2 binary reflective optical switch fabricated using SOI wafers and DRIE. An electrostatic comb actuator controls the position of a micromirror. In the cross state, light from an input fiber is deflected by 90º. In the bar state, the light from that fiber travels unobstructed through the switch. Side schematics illustrate the signal path for each state. The typical response time is 500 μs.

Проекционные дисплеи Projectors

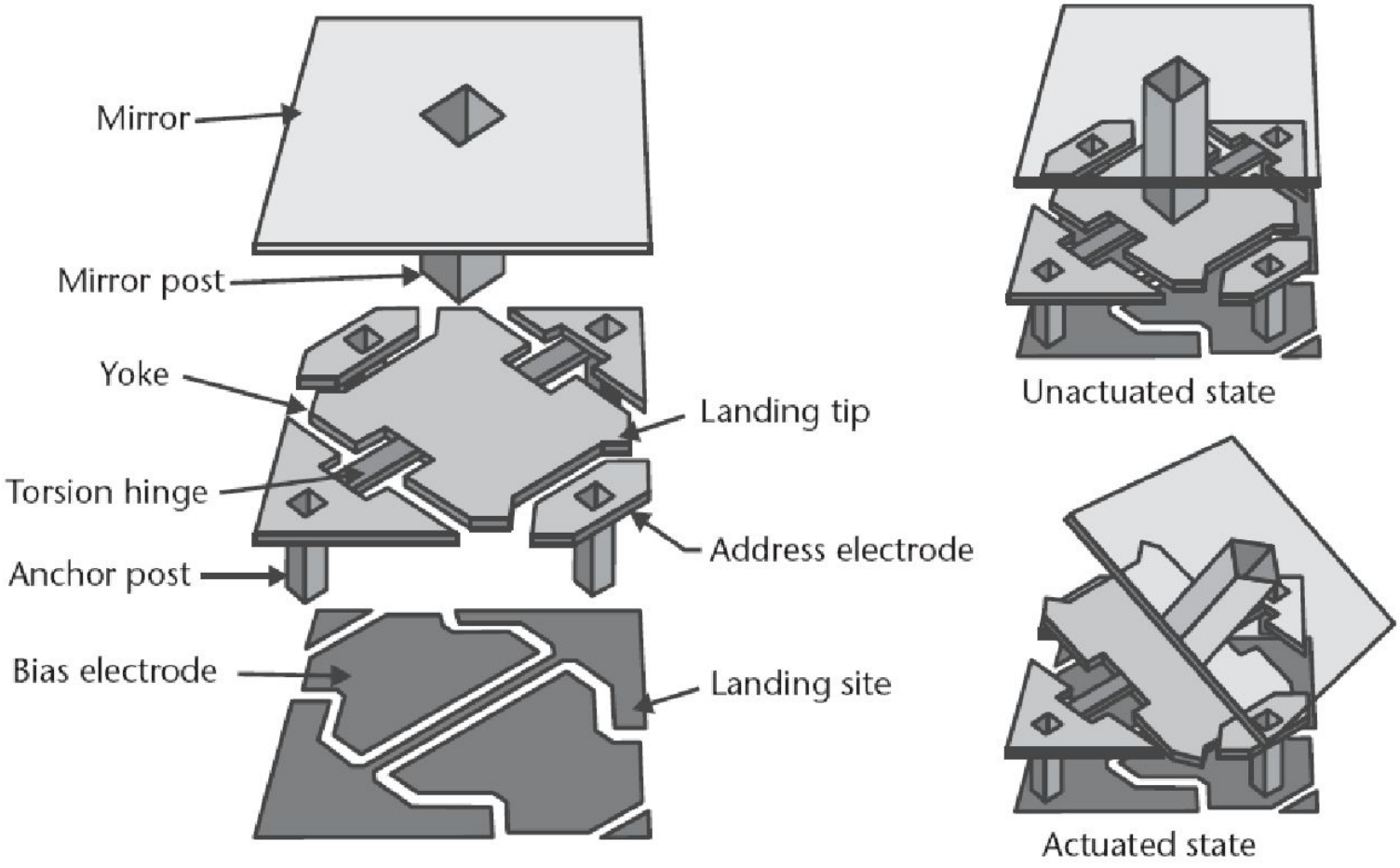

Illustration of a single DMD pixel in its resting and actuated states. The basic structure consists of a bottom aluminum layer containing electrodes, a middle aluminum layer containing a yoke suspended by two torsional hinges, and a top reflective aluminum mirror. An applied electrostatic voltage on a bias electrode deflects the yoke and the mirror towards that electrode.

Микрозеркала Micromirrors

Each micromirror is 16 μm square and is made of aluminum. The pixels are normally arrayed in two dimensions on a pitch of 17 μm to form displays with standard resolutions from 800 x 600 pixels (SVGA) up to 1,280x1,024 pixels (SXGA). The fill factor is approximately 90%. The mechanical switching time is 16 μs.

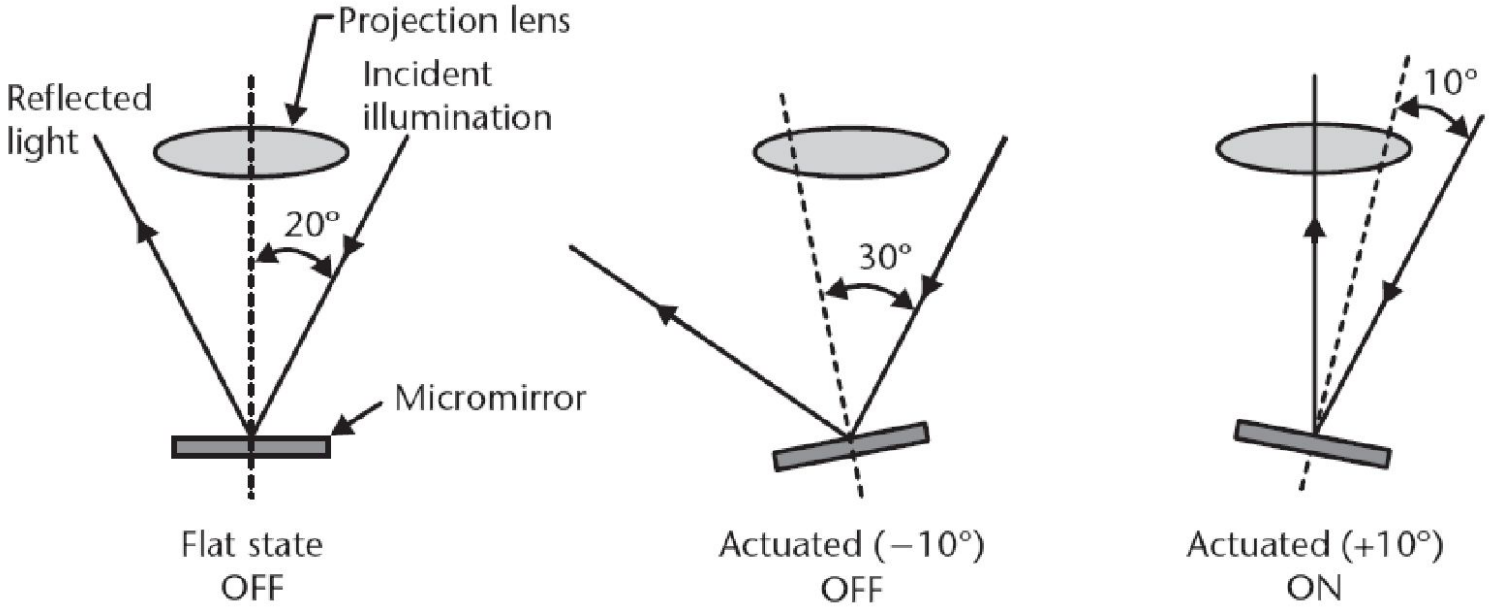

Illustration of optical beam steering using the switching of micromirrors. Off-axis illumination reflects into the pupil of the projection lens only when the micromirror is tilted in its +10º state, giving the pixel a bright appearance. In the other two states, the pixel appears dark.

Микрозеркало - последовательность производства
Micromirror fabrication steps

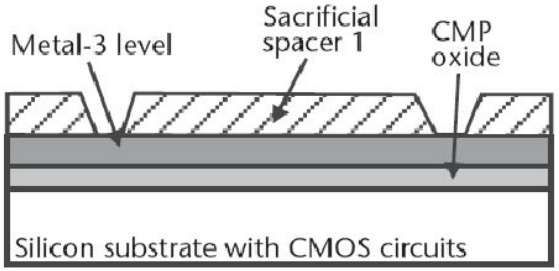

1. Pattern spacer 1 layer

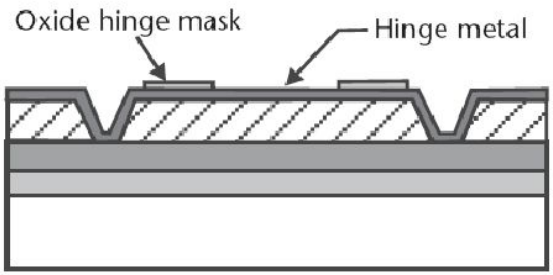

2. Deposit hinge metal; deposit and pattern oxide hinge mask

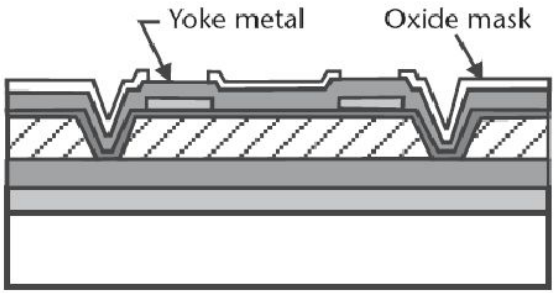

3. Deposit yoke and pattern yoke oxide mask

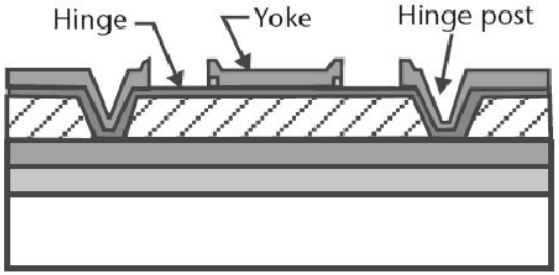

4. Etch yoke and strip oxide

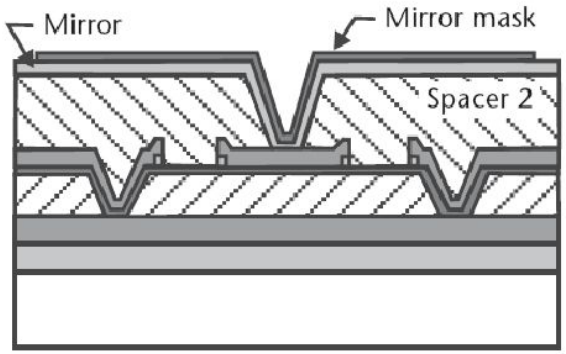

5. Deposit spacer 2 and mirror

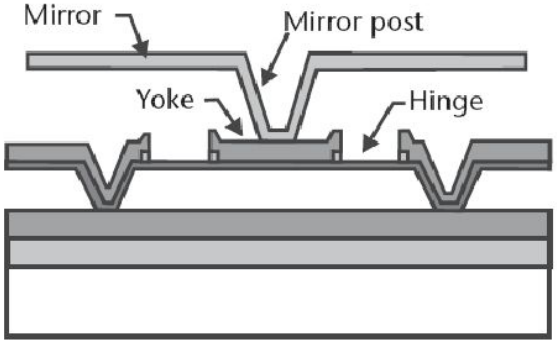

6. Pattern mirror and etch sacrificial spacers

Дифракционный оптический переключатель
Optical diffraction switch

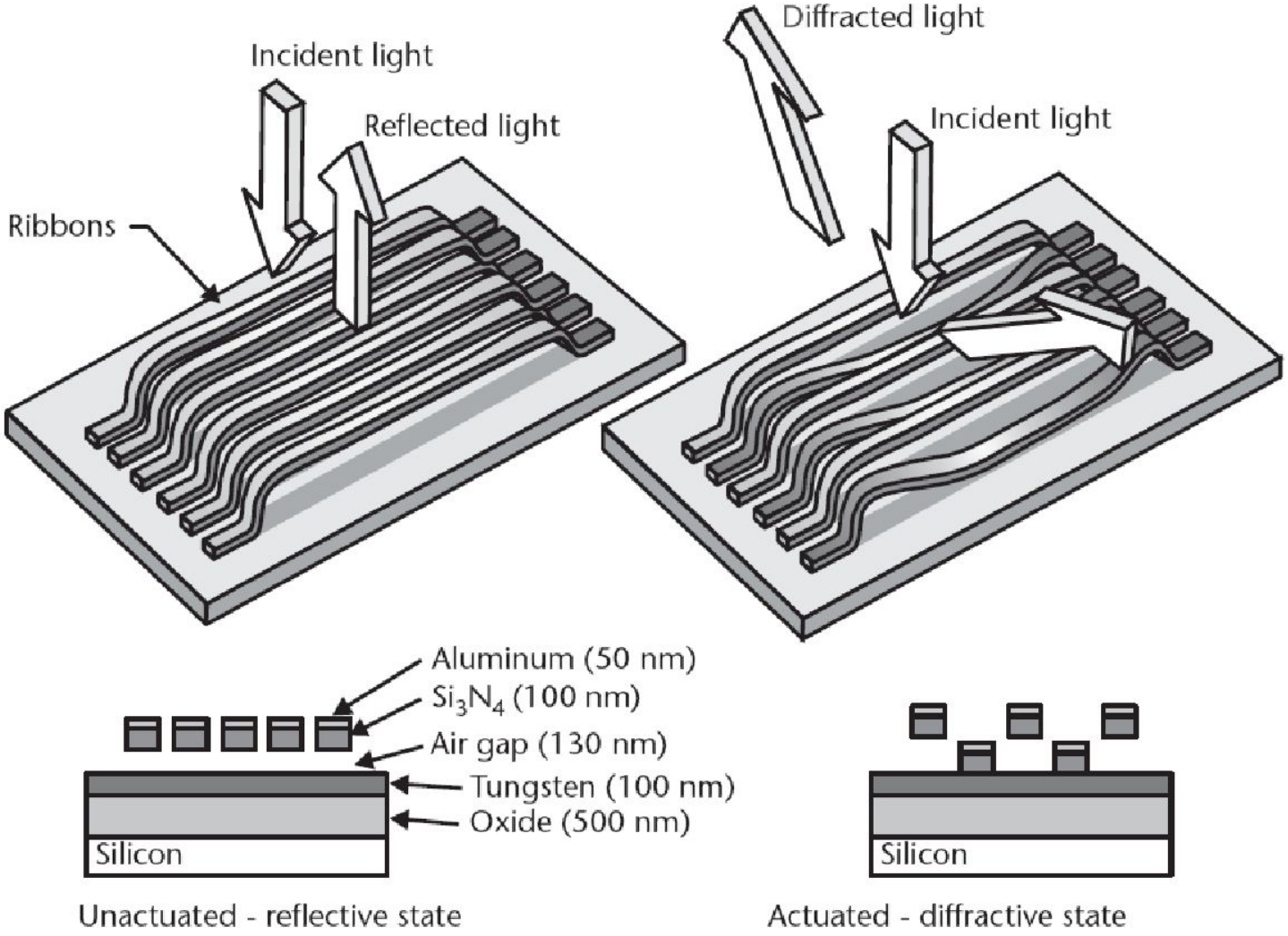

Illustration of the operating principle of a single pixel in the GLV. Electrostatic pull down of alternate ribbons changes the optical properties of the surface from reflective to diffractive.

Цветной проекционный элемент Color projection

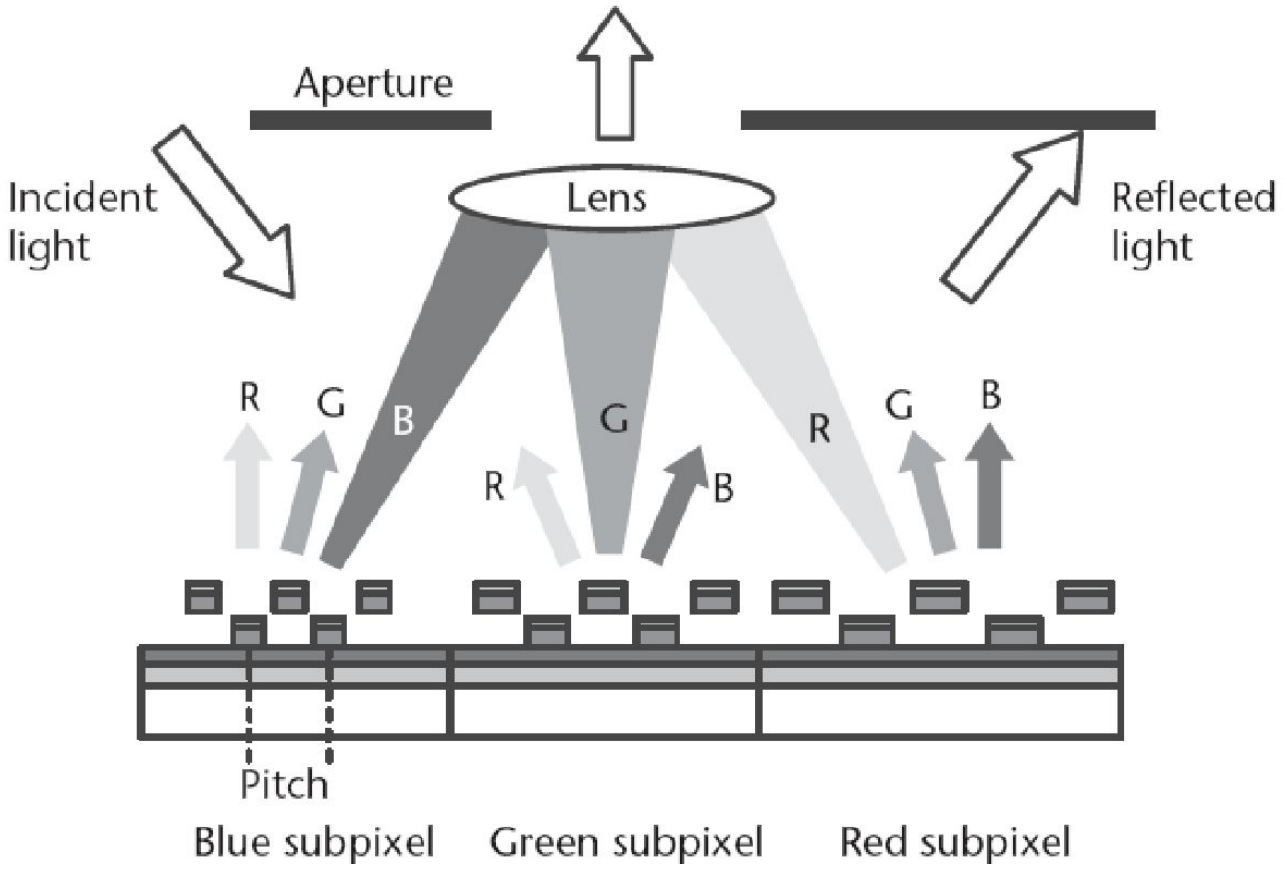

Implementation of color in a GLV pixel. The pitch of each color subpixel is tailored to steer the corresponding light to the projection lens. The aperture blocks the reflected light but allows the first diffraction order to enter the imaging optics. The size of the pixel is exaggerated for illustration purposes. Switching speed is about 20 ns.

Перестраиваемый лазер Tunable laser

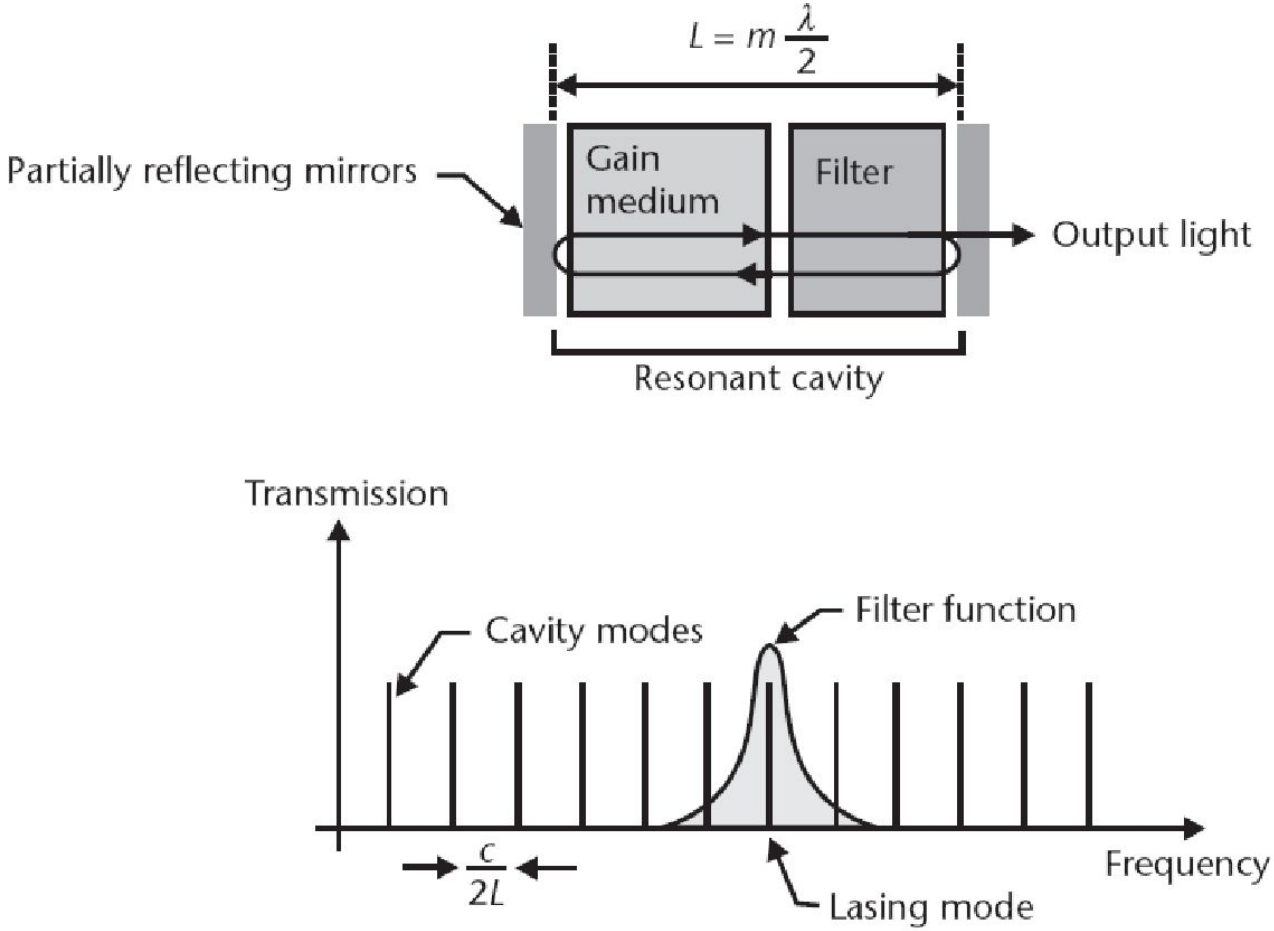

Illustration of the building blocks of a laser. A gain medium amplifies light as it oscillates inside a resonant cavity. Only select wavelengths called longitudinal cavity modes that are separated by a frequency equal to $c/2L$ may exist within the cavity. A wavelength filter with a narrow transmission function selects one lasing mode and ensures that the output light is monochromatic.

Внешний резонатор для перестраиваемого лазера
External resonator for a tunable laser

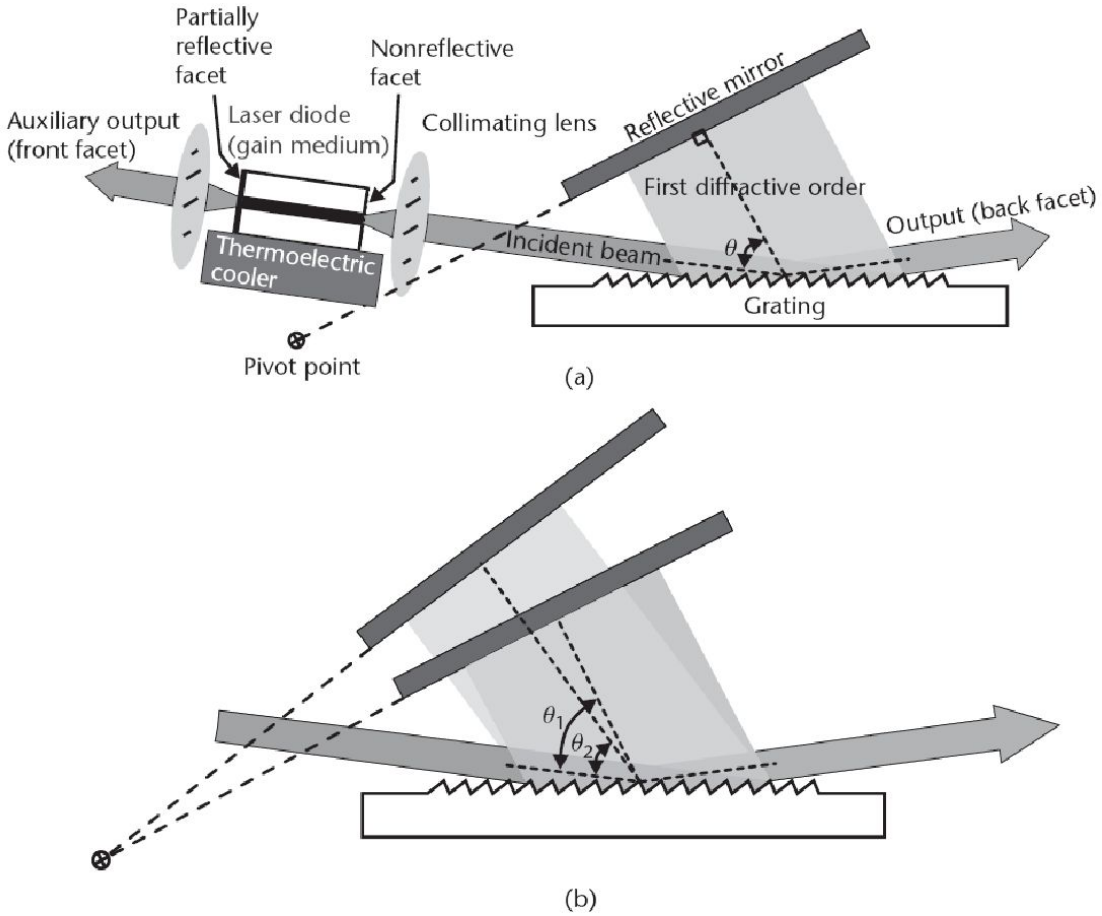

(a) Illustration of the Littman-Metcalf external cavity laser configuration. Light from the laser diode is collimated and diffracted by a grating acting as a wavelength filter. Lasing occurs only at one wavelength, whose diffraction order is reflected by the mirror back into the cavity. (b) Rotating the mirror around a virtual pivot point changes the wavelength and tunes the laser.

Массив лазеров и оптоволокно
Collimation of a laser from array into an optical fiber

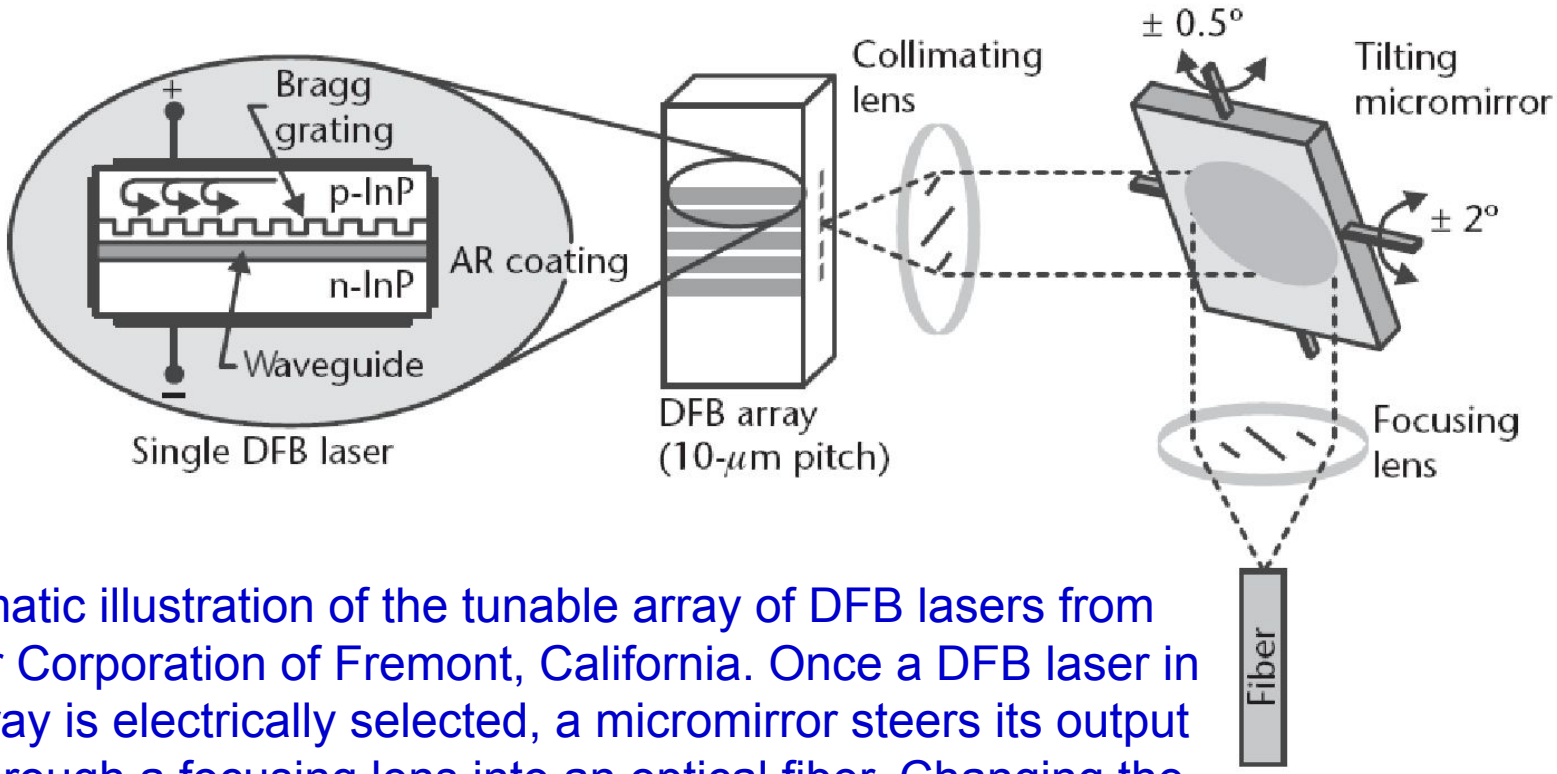

Schematic illustration of the tunable array of DFB lasers from Santur Corporation of Fremont, California. Once a DFB laser in the array is electrically selected, a micromirror steers its output light through a focusing lens into an optical fiber. Changing the temperature of the DFB laser array using a TEC device tunes the wavelength over a narrow range. The illustration on thefar left depicts the simplified internal structure of a single DFB laser. Both facets of the semiconductor diode are coated with an antireflection (AR) coating.

Микрозеркало Micromirror

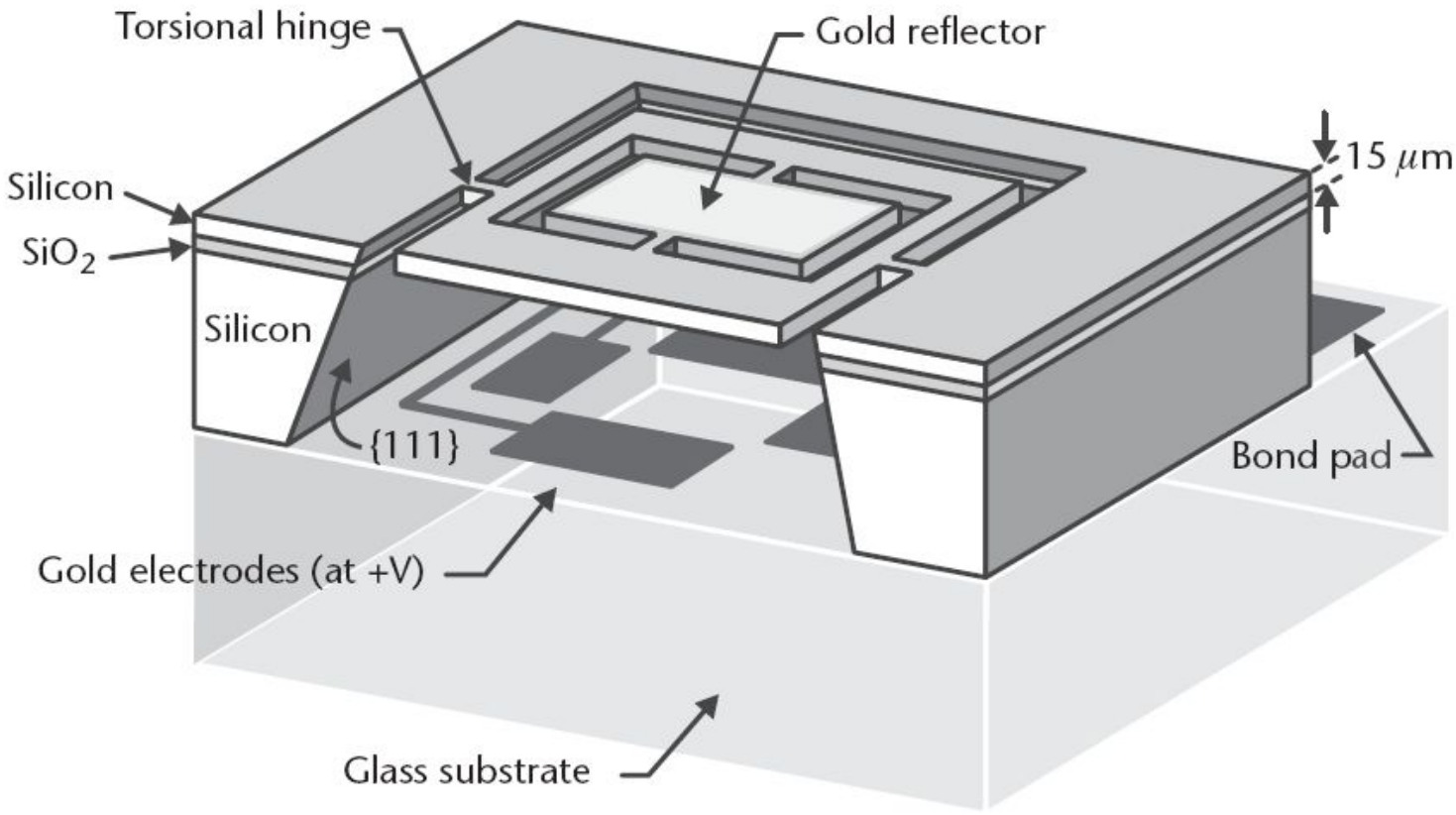

Schematic cross section of the micromirror used within the tunable laser from Santur Corporation. The device consists of a double-gimbaled mirror structure supported by torsional hinges. A gold layer defines the high-reflectivity mirror surface that remains at ground potential. Four gold electrodes on an anodically bonded glass substrate actuate the mirror and cause rotation around the hinges.

Многоканальный оптический переключатель
Multichannel optical switch

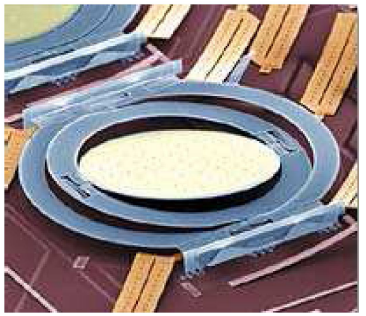

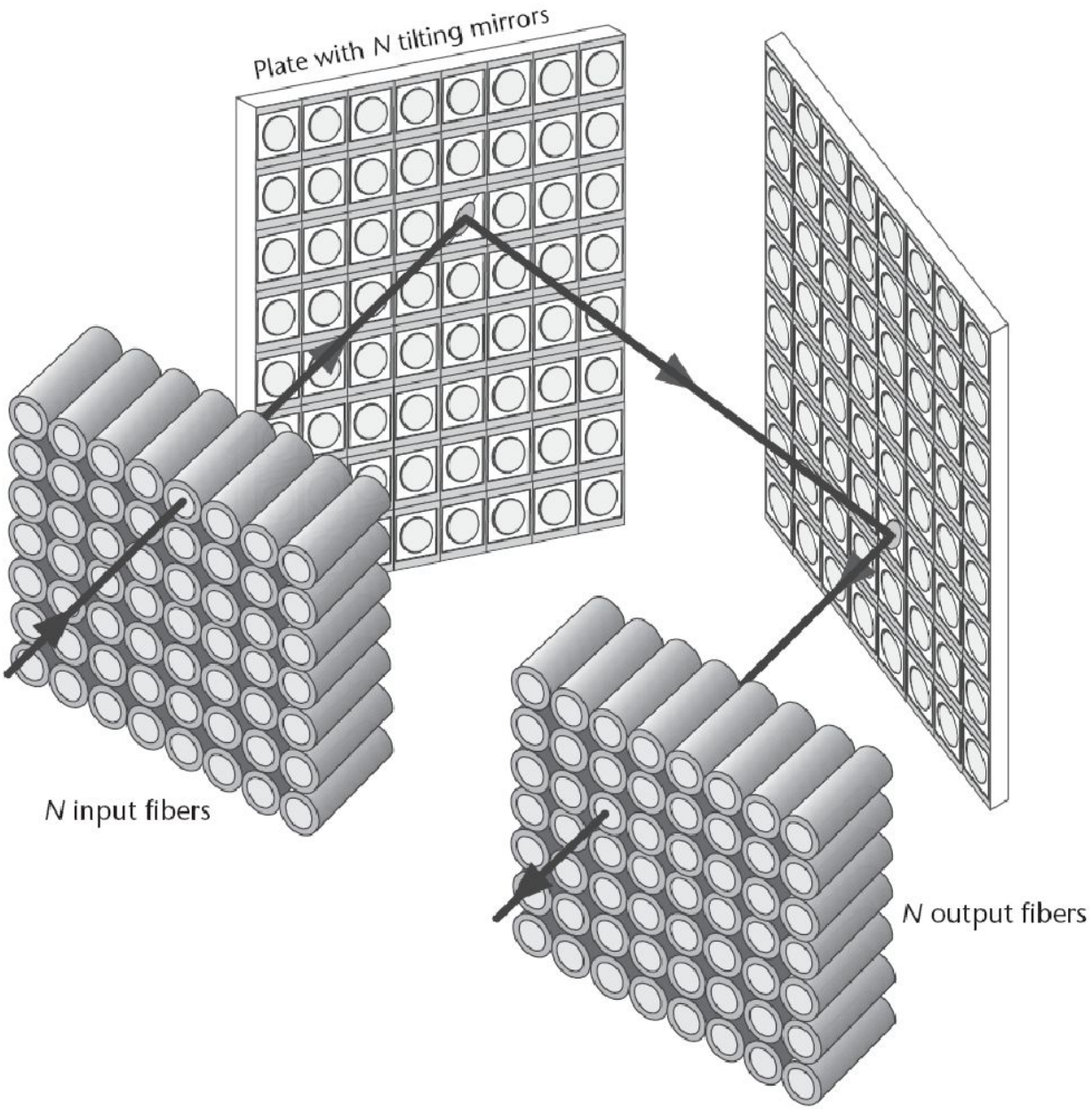

Schematic illustration of the 3-D architecture for an *N* x *N* switch or photonic cross connect. A beam-steering micromirror on a first plate points the light from a collimated input fiber to another similar micromirror on a second plate, which in turn points it to a collimated output fiber. This system architecture requires a total of 2*N* continuously tilting mirrors in two directions. To minimize the maximum angular displacement of the mirrors, the two plates are positioned at 45º relative to the incident light.

Замещение пассивных электронных элементов
Replacement of passive electronic components

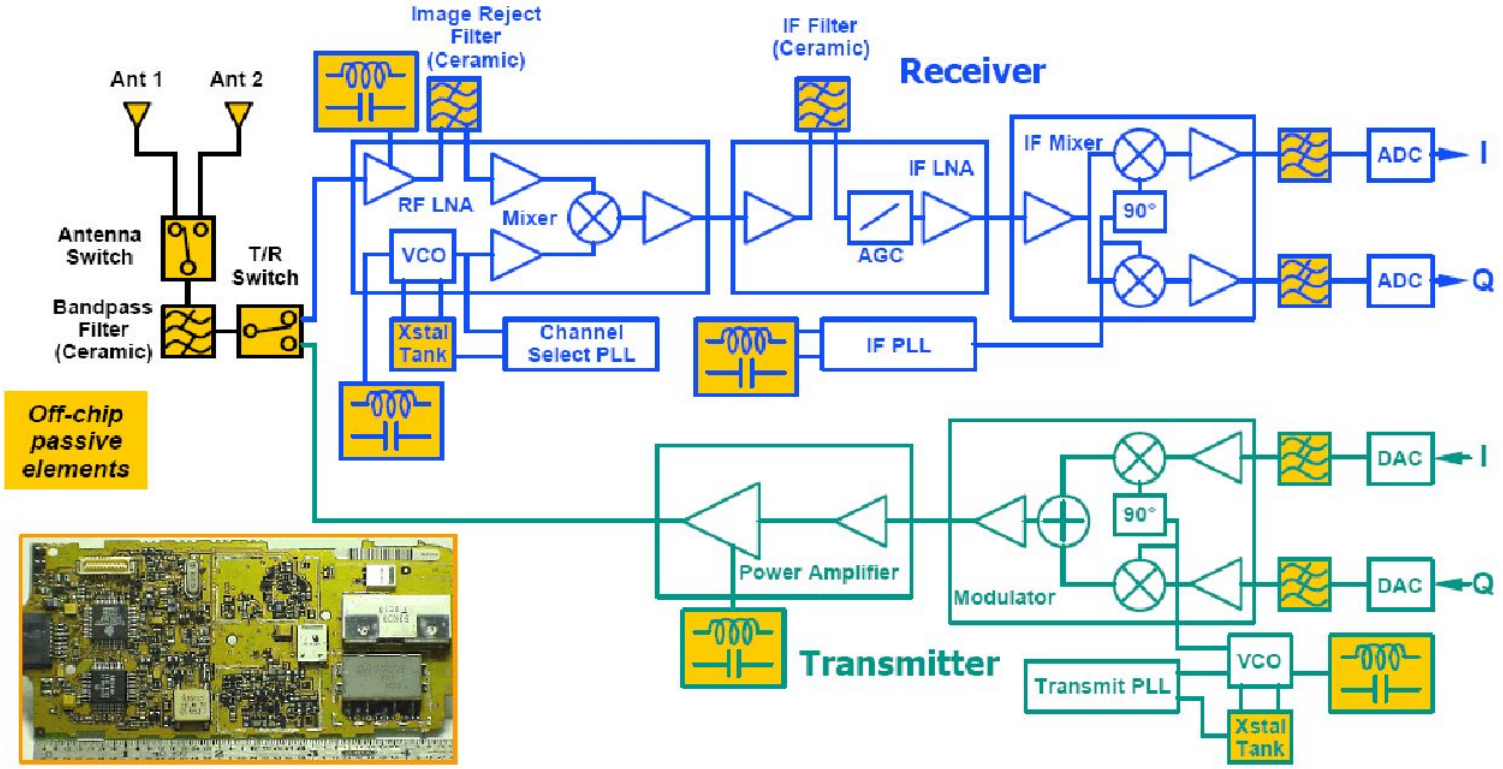

Current Cell Phone Board
Off-chip C & L = 80% of area

Current research:

- ✓ **Replace all off-chip passive elements with MEMS resonators & filters ⇒ chip-scale integration & improved performance**

Индуктивность Microinductor

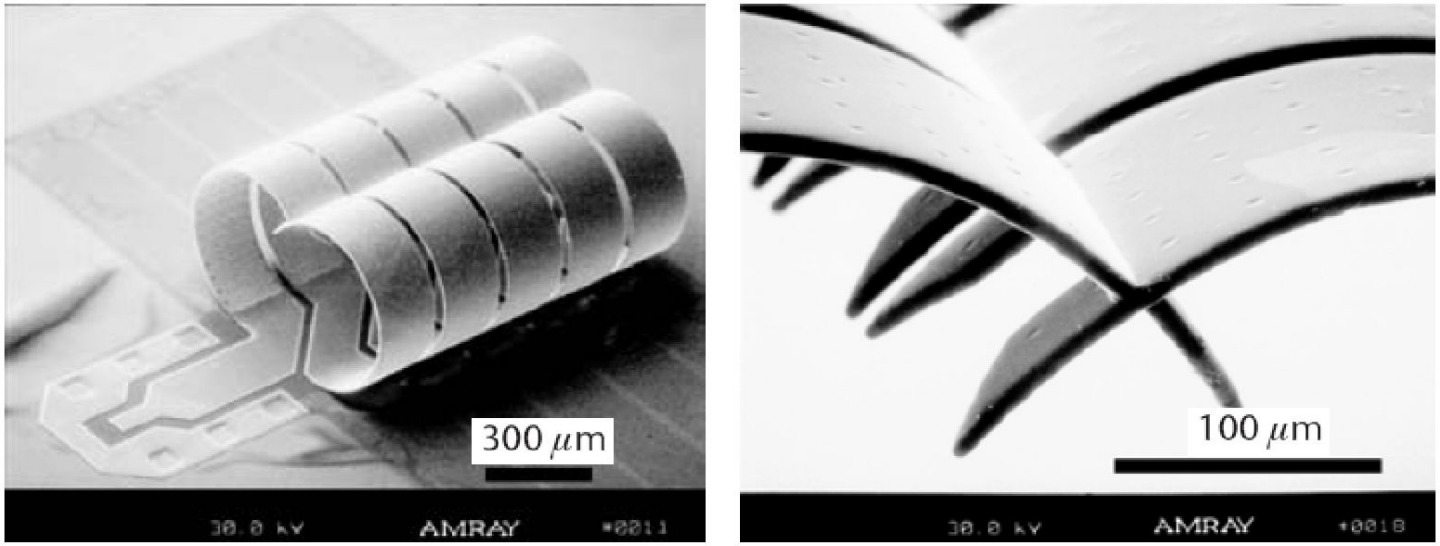

(a) (b)

The PARC inductor: (a) scanning-electron micrograph (SEM) of a five-turn solenoid inductor (the locations of the sides of the turns before release are visible); and (b) SEM close up of the tops of the turns where the metal from each side meets, showing the interlocked ends. The etch holes have been filled with copper.

Индуктивность - последовательность производства НЭМС Fabrication of microinductor

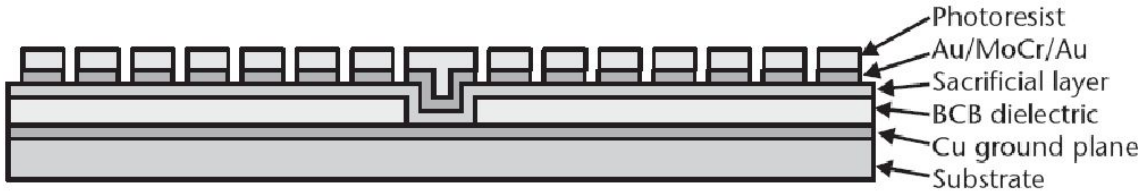

1. Deposit Cu ground plane. Deposit and pattern dielectric.
Sputter sacrificial metal and Au/MoCr/Au stack with stress gradient in MoCr.
Pattern metal with photoresist and etch.

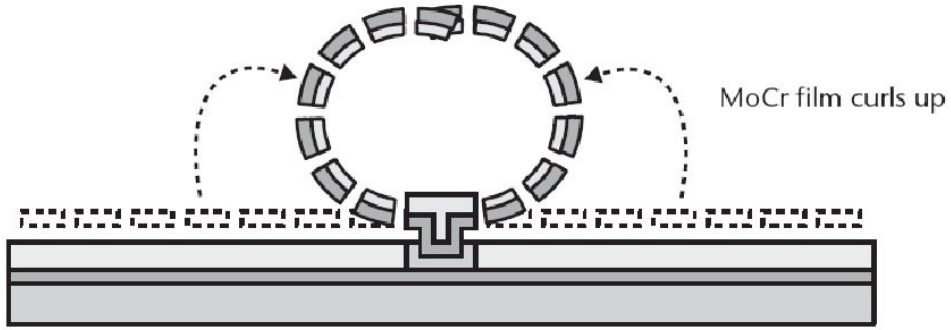

2. Etch sacrificial layer to release MoCr film, which curls slightly.
Heat to relax photoresist. Au/MoCr/Au stack curls completely.

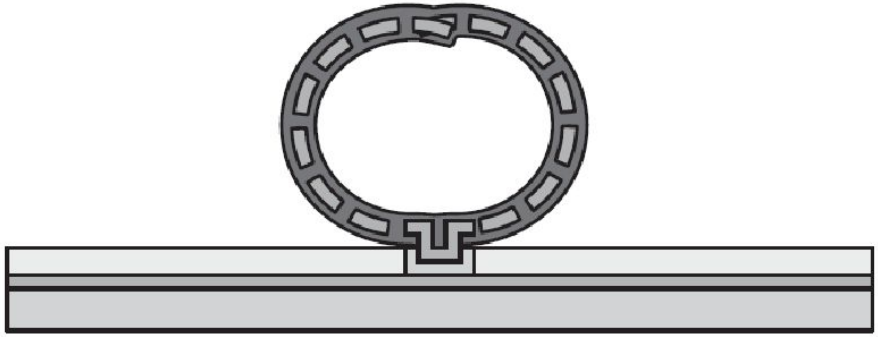

3. Strip photoresist.
Electroplate Au/MoCr/Au with copper.

Переменная емкость Tunable capacitor

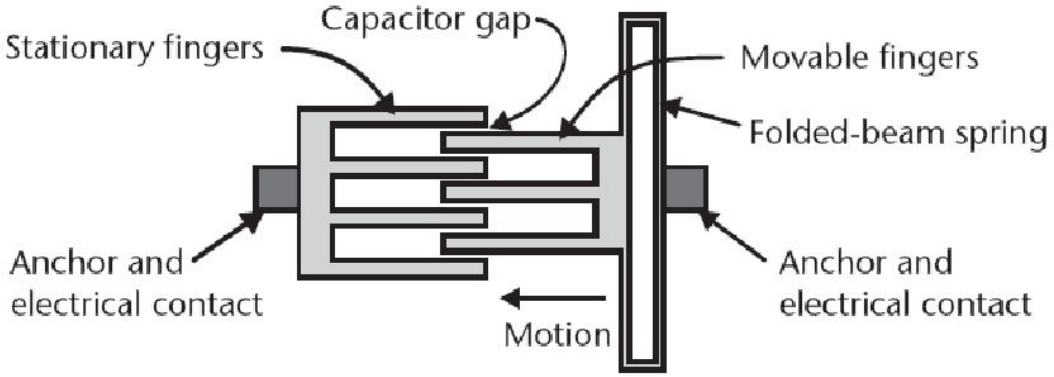

(a)

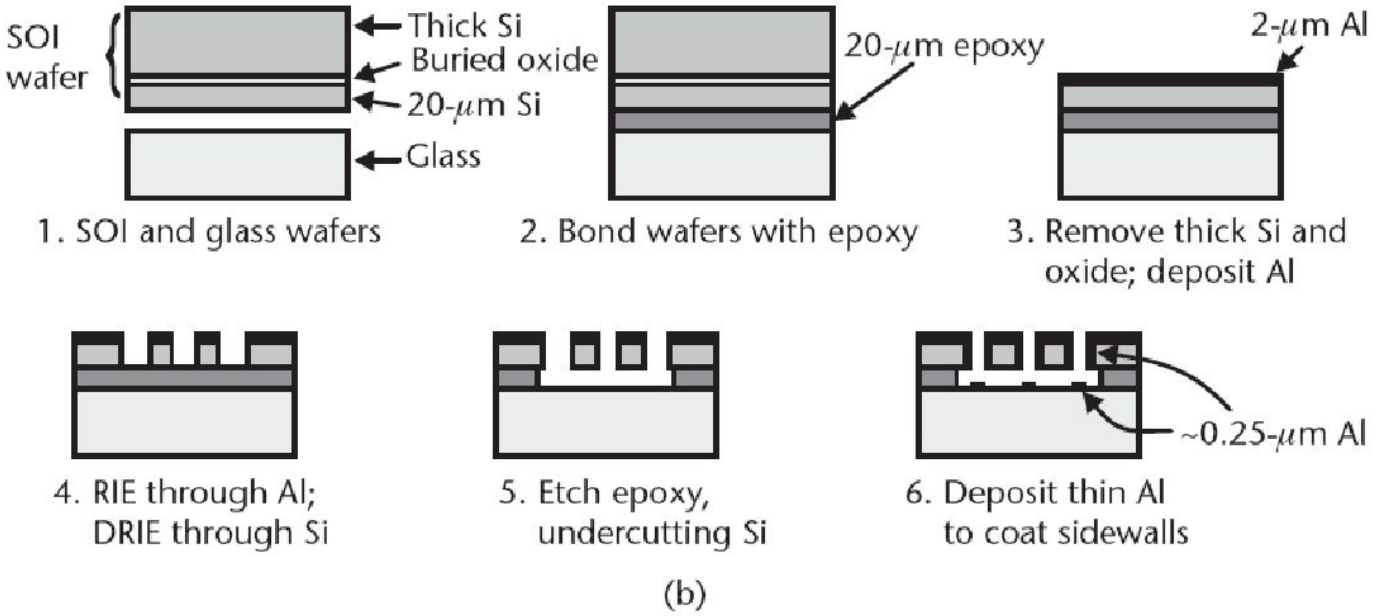

(b)

Резонатор Resonator

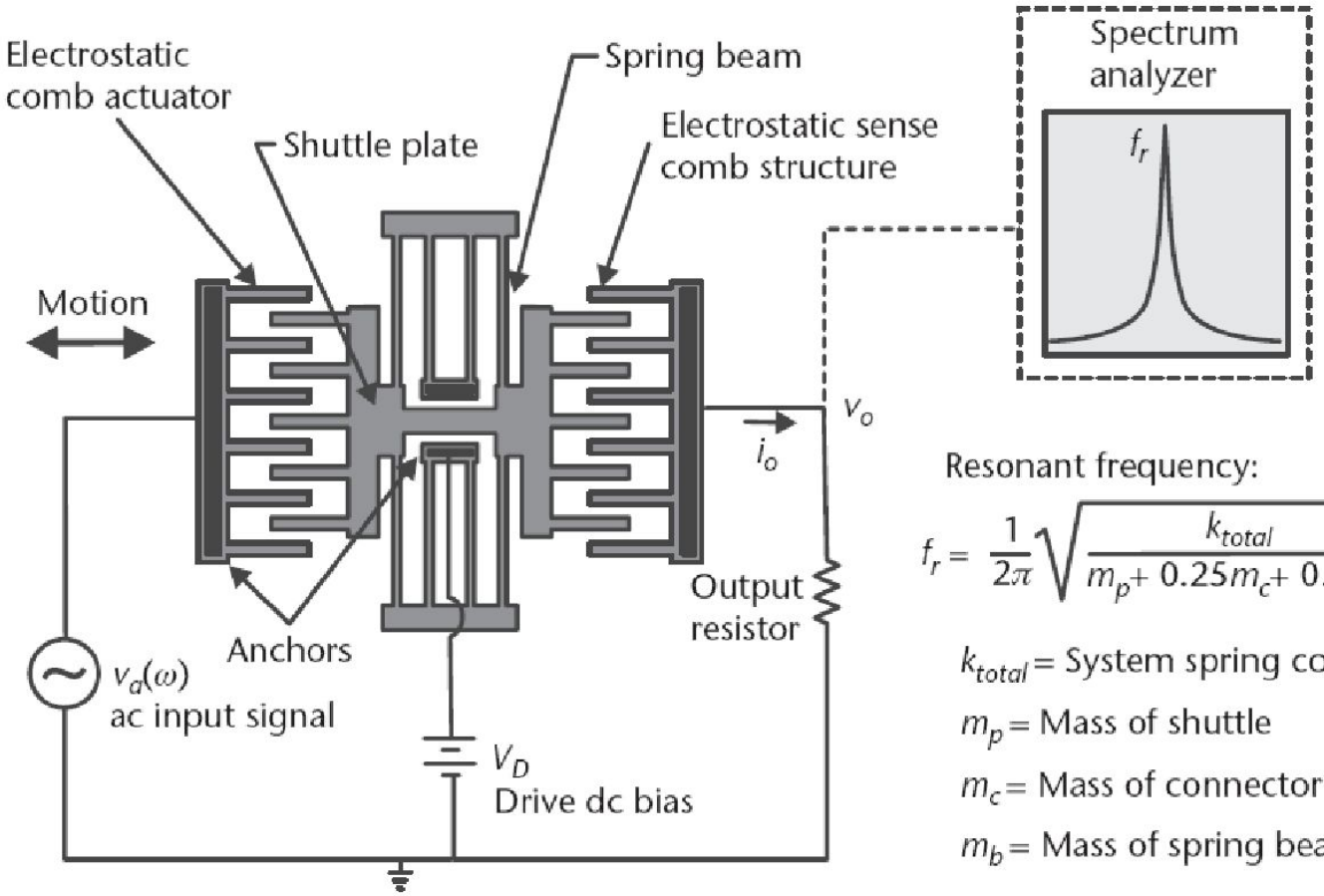

Resonant frequency:

$$f_r = \frac{1}{2\pi}\sqrt{\frac{k_{total}}{m_p + 0.25m_c + 0.34m_b}}$$

k_{total} = System spring constant

m_p = Mass of shuttle

m_c = Mass of connector

m_b = Mass of spring beams

Добротность Q

кварц Q≈10000

RLC Q<1000

НЭМС:

вакуум Q>50000

воздух Q<50

$k = E\,t\,(w/L)^3$

E = 160 GPa

t = 2 μm

w = 2 μm

L = 33 μm

$m = 5.7\ 10^{-11}$ kg

f = 190 kHz

Illustration of a micromachined folded-beam comb-drive resonator. The left comb drive actuates the device at a variable frequency ω. The right capacitive-sense-comb structure measures the corresponding displacement by turning the varying capacitance into a current, which generates a voltage across the output resistor. There is a peak in displacement, current, and output voltage at the resonant frequency.

Высокочастотный резонатор с термокомпенсацией
Resonator with thermal compensation

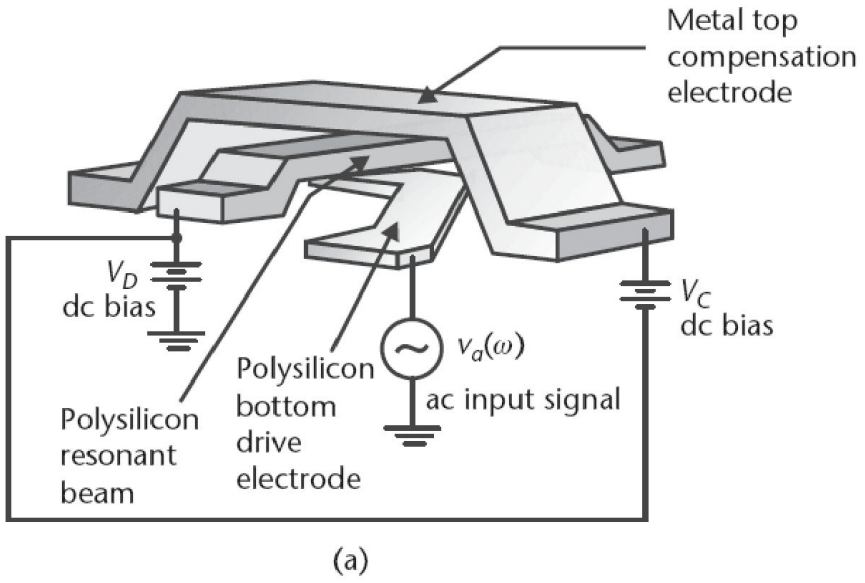

(a)

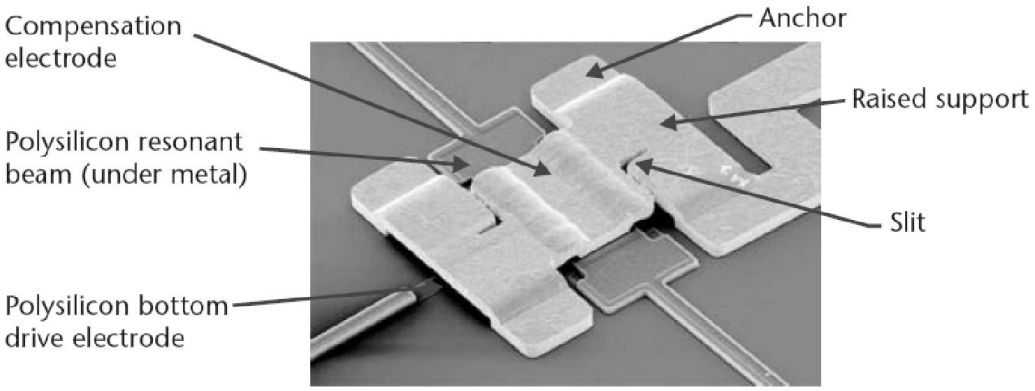

(b)

Illustration of the compensation scheme to reduce sensitivity in a resonant structure to temperature. A voltage applied to a top metal electrode modifies through electrostatic attraction the effective spring constant of the resonant beam. Temperature changes cause the metal electrode to move relative to the polysilicon resonant beam, thus changing the gap between the two layers. This reduces the electrically induced spring constant opposing the mechanical spring while the mechanical spring constant itself is falling, resulting in their combination varying much less with temperature. (a) Perspective view of the structure, and (b) scanning electron micrograph of the device. (*Courtesy of:* Discera, Inc., Ann Arbor, Michigan, USA.)

Переключатель Electric switch

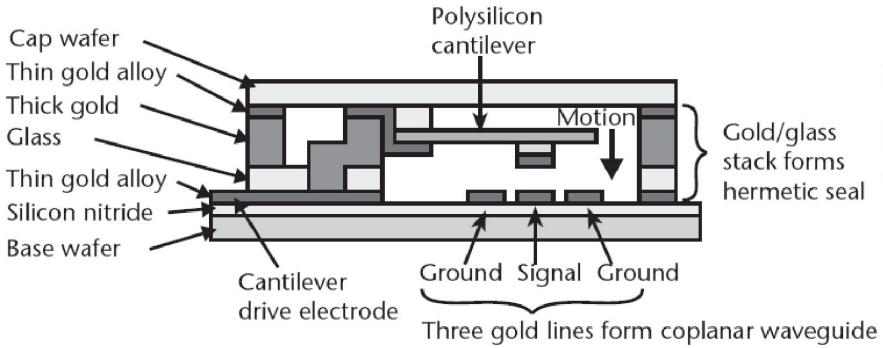

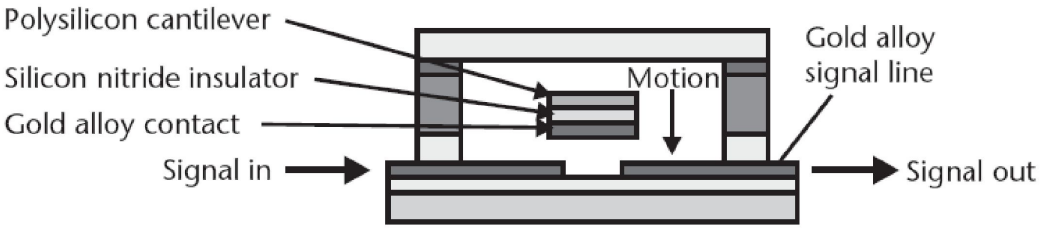

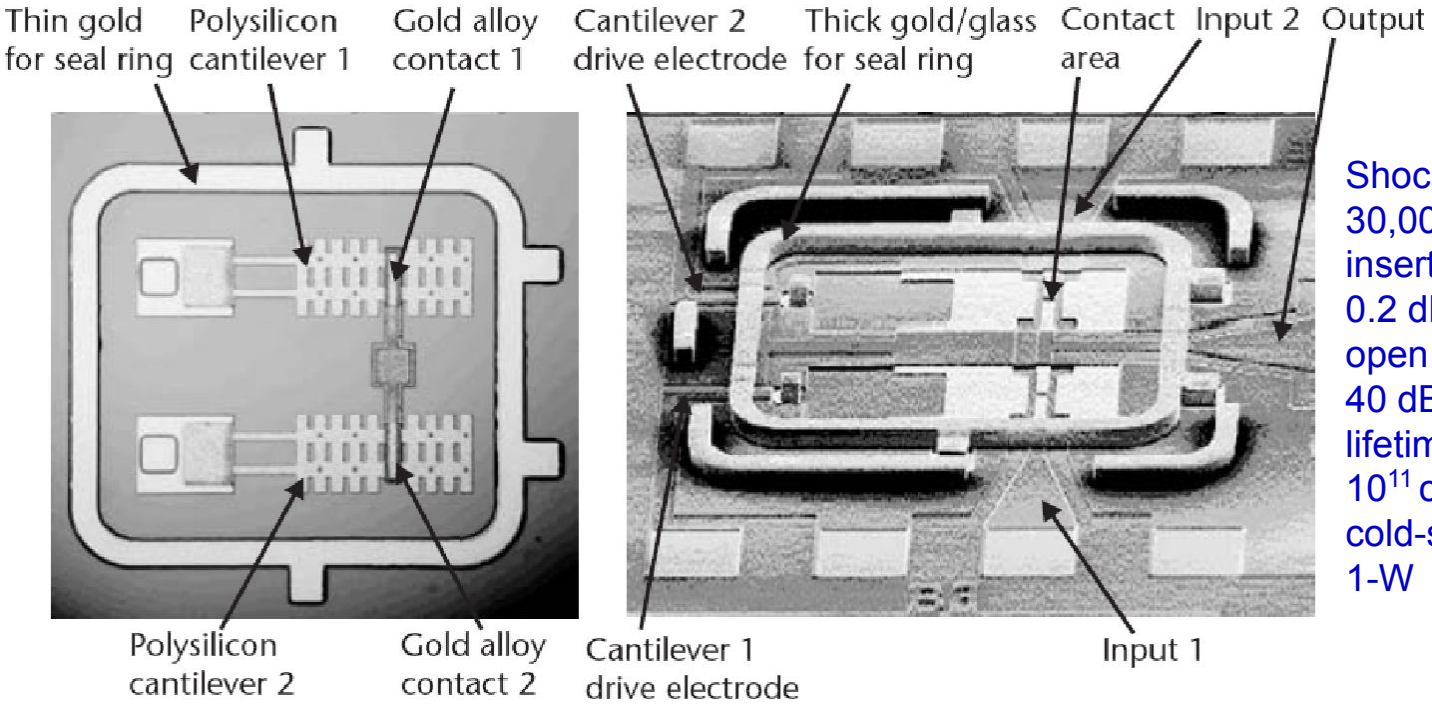

Shock tolerance of 30,000G, insertion loss of 0.2 dB over 24–40 GHz, open isolation of 40 dB, lifetime of 10^{11} cycles, cold-switched power of 1-W

MicroAssembly Technologies of Richmond, California, USA

To be continued

Домашнее задание

...